

**PERFORMANCE OF WRF IN SIMULATING THE HAIL EVENT
OVER ISTANBUL ON 27 JULY 2017**

M.Sc. THESIS

Emir TOKER

Climate and Marine Sciences Department

Earth System Science Program

JUNE 2018

**PERFORMANCE OF WRF IN SIMULATING THE HAIL EVENT
OVER ISTANBUL ON 27 JULY 2017**

M.Sc. THESIS

**Emir TOKER
(601151011)**

Climate and Marine Sciences Department

Earth System Science Program

Thesis Advisor: Prof. Dr. Ömer Lütfi ŞEN

JUNE 2018

**27 TEMMUZ 2017 TARİHİNDE İSTANBUL ÜZERİNDE MEYDANA GELEN
DOLU OLAYININ WRF SİMÜLASYONU PERFORMANSI**

YÜKSEK LİSANS TEZİ

**Emir TOKER
(601151011)**

İklim ve Deniz Bilimleri Anabilim Dalı

Yer Sistem Bilimleri Programı

Tez Danışmanı: Prof. Dr. Ömer Lütfi ŞEN

HAZİRAN 2018

Emir TOKER, a M.Sc. student of ITU Eurasia Institute of Earth Sciences Climate and Marine Sciences 601151011 successfully defended the thesis entitled “PERFORMANCE OF WRF IN SIMULATING THE HAIL EVENT OVER ISTANBUL ON 27 JULY 2017”, which he/she prepared after fulfilling the requirements specified in the associated legislations, before the jury whose signatures are below.

Thesis Advisor : **Prof. Dr. Ömer Lütfi ŞEN**
Istanbul Technical University



Jury Members : **Prof. Dr. Hasan Nüzhet DALFES**
Istanbul Technical University



Prof. Dr. Mete TAYANÇ
Marmara University



.....

Date of Submission : 4 May 2018
Date of Defense : 6 June 2018

To my family and friends,

FOREWORD

This work is about an extreme weather events and atmospheric modelling. The hail event that took place in Istanbul on 27 July 2017 is defined as the study case. It is aimed to improve the hail simulation by trying different physics options available in the WRF model. I hope my study contributes to understanding and prediction of hail events.

I would like to thank to my advisor Prof. Dr. Ömer Lütfi ŞEN for guiding me in my study. My special thanks go to Res. Asst. Dr. Yasemin EZBER for helping me in setting up and running the WRF model. Endless thanks to my family who supports me materially and morally.

June 2018

Emir TOKER

TABLE OF CONTENTS

	<u>Page</u>
FOREWORD	ix
TABLE OF CONTENTS	xi
ABBREVIATIONS	xiii
SYMBOLS	xv
LIST OF TABLES	xvii
LIST OF FIGURES	xix
SUMMARY	xxi
ÖZET	xxiii
1. INTRODUCTION	1
1.1 Structure and Formation of Hail.....	1
1.2 Literature Review	2
1.3 Objectives	4
2. DATA	5
2.1 Observation Data	5
2.2 Re-Analysis Data.....	5
3. INVESTIGATION OF 7 JULY 2017 HAIL EVENTI	7
3.1 Case Description.....	7
3.2 Synoptic Situation	15
4. MODEL	21
4.1 The WRF Model.....	21
4.2 Model Setup.....	21
4.2.1 Study area	22
4.2.2 The physics schemes	23
4.3 Post-Processing.....	24
5. RESULTS	25
5.1 Performance of the Model	25
5.1.1 Sensitivity study with different microphysics schemes.....	27
5.1.2 Sensitivity study with different cumulus schemes.....	29
5.1.3 Sensitivity study with different planetary boundary layer schemes	30
5.1.4 Sensitivity study with different radiation schemes	32
5.2 Analysis of the Model Outputs.....	32
6. SUMMARY AND CONCLUSION	41
REFERENCES	43
APPENDICES	47
CURRICULUM VITAE	55

ABBREVIATIONS

Cb	: Cumulonimbus
WRF	: Weather Forecasting Research
WPS	: WRF Preprocessing System
US	: United States
PBL	: Planetary Boundary Layer
TSMS	: Turkish State Meteorological Service
AWOS	: Automated Weather Observing System
ECMWF	: European Center for Medium-Range Weather Forecasts
NCAR	: The National Center for Atmospheric Research
ARW	: Advanced Research WRF
NMM	: Nonhydrostatic Mesoscale Model
MODIS	: Moderate Resolution Imaging Spectroradiometer
GLCF	: The Global Land Cover Facility
USD	: United States Dollar
UTC	: Coordinated Universal Time
3D	: Three-dimensional
MYNN	: Mellor-Yamada Nakanishi Niino
NCEP	: National Centers for Environmental Prediction
FNL	: Final
TMPA	: Tropa Satellite Rainfall Measurement - Analysis
WSM	: WRF Single-Moment
RRTM	: Rapid radiative transfer model
YSU	: Yonsei University
KF	: Kain Fritsch
CuP	: Cumulus potential
MS	: Multi-scale

SYMBOLS

C	: Celcius
m	: Meter
mm	: Millimeter
kg	: Kilogram
°	: Degree
%	: Percent
mb	: Millibar
h	: Hour
hPa	: Hectopascal
km	: Kilometer
s	: Second
dBZ	: Decibels of Z
g	: Gram
m³	: Cubic meter
gpdam	: Geopotential height-Decametre

LIST OF TABLES

	<u>Page</u>
Table 3.1 : Weather event types and times (UTC) of occurrence and station informations	7
Table 5.1 : Experiment numbers and options	26
Table 5.2 : Experiments and specified options for microphysics comparing.....	27
Table 5.3 : Experiment numbers and options for cumulus	29
Table 5.4 : Experiment numbers and options for planetary boundary layer	31
Table 5.5 : Experiment numbers and options for cumulus	32

LIST OF FIGURES

	<u>Page</u>
Figure 3.1 : Cloudiness, satellite images on 27.07.2017.	8
Figure 3.2 : Cloud top temperature, satellite images on 27.07.2017.	9
Figure 3.3 : Accumulated rain, 1-hour, radar images on 27.07.2017.	10
Figure 3.4 : Wind, radar images on 27.07.2017.	11
Figure 3.5 : Reflectivity, radar images on 27.07.2017.	12
Figure 3.6 : Station names, locations and terrain height of inner domain.	13
Figure 3.7 : Between 27.07.2017 00:00 UTC and 28.072017 00:00 UTC with 15 minutes interval time step, times series for 11 stations.	14
Figure 3.8 : Era-Interim, surface pressure (hPa) (4 mb interval contours) and jet stream (km/hour) in 300 hPa pressure level. 26.07.2017 12:00 UTC and 28.07.2017 00:00 UTC with 12-hour time interval.	16
Figure 3.9 : Era-Interim, geopotential height (gpdam) and winds (km/h) in 500 hPa. 26.07.2017 12:00 UTC and 28.07.2017 00:00 UTC with 12-hour time interval.	18
Figure 3.10 Era-Interim, mean sea level pressure (hPa) (4 mb interval contours) and relative vorticity ($10E-5/s$) in 300 hPa. 26.07.2017 12:00 UTC and 28.07.2017 00:00 UTC with 12-hour time interval.	19
Figure 4.1 : Domains and terrain (m).	23
Figure 5.1 : Cloud top temperature($^{\circ}C$), hail(mm) and accumulated rain(mm) for microphysics schemes on July 27, 2017 at 14:15 UTC.	28
Figure 5.2 : Cloud top temperature($^{\circ}C$), hail(mm) and accumulated rain(mm) for cumulus schemes on July 27, 2017 at 14:15 UTC.	30
Figure 5.3 : Cloud top temperature($^{\circ}C$), hail(mm) and accumulated rain(mm) for planetary boundary layers schemes on July 27, 2017 at 14:15 UTC.	31
Figure 5.4 : Cloud top temperature($^{\circ}C$), hail(mm) and accumulated rain(mm) for radiation schemes on July 27, 2017 at 14:15 UTC.	33
Figure 5.5 : Model results on 11 stations coordinates between 27.07.2017 00:00 UTC and 28.072017 00:00 UTC with 15 minutes interval time step.	34
Figure 5.6 : Bakırköy region between 27.07.2017 00:00 UTC and 28.072017 00:00 UTC with 15 minutes interval time step.	35
Figure 5.7 : Terrain height(m) and cross-section line for the best model simulation on July 27, 2017 at 14:15 UTC.	36
Figure 5.8 : Relative Humidity, Temperature ($^{\circ}C$) contours of cross-section for the best model simulation on July 27, 2017 at 14:15 UTC.	37
Figure 5.9 : 3D plot of air movement direction on July 27, 2017 at 14:15 UTC. .	39

Figure 5.10 3D cloudiness(0-1), accumulated hail(mm) for the best model simulation on July 27, 2017 at 14:15 UTC. 40

PERFORMANCE OF WRF IN SIMULATING THE HAIL EVENT OVER ISTANBUL ON 27 JULY 2017

SUMMARY

Hail development is a very regional and short-term consequence. Therefore, hail is one of the most difficult predictable meteorological event. Nowadays, it is possible to predict it with remote sensing and short-term forecasting tools. After the increase of the computing capacity of the computers, in the studies, high-performance computers and improved weather forecasting models are used, and the efficiency of weather forecast methods is analyzed by comparing observations with model outputs. Physics options in the model are modified according to facts and characteristics of the event and the simulations are run in order to predict the meteorological phenomenon close to real weather event using different parametrization.

The water droplets in the deep convective clouds are transported to the higher levels by means of ascending and descending air movements. Water droplets cool down at these higher levels and become ice particles. As a result of the repetition of the vertical transport in the cloud, the ice particle become larger. They fall when they defeat the gravity force.

Several extreme weather events took place in Istanbul in July 2017. The heavy hail event on July 27 damaged hundreds of buildings and thousands of vehicles. The cost of this hazardous event was estimated to be around 300 Million US Dollars. As a result of these weather events, the total precipitation was recorded as of 30-40 kg.

In the Northern Hemisphere, jets emerging in the middle and upper latitudes and as a result of the pressure systems that have been strengthened over Europe, there has been ascending air movements, including the Thracian region, and vertical clouds have formed. This system has been effective for some time. The study area includes the area where the hail event has occurred and is effective. Istanbul region is positioned in the centre of the study area. Area information, initial and boundary conditions are identified with the data and model is run for hail model simulations.

The state-of-the-art Weather Research and Forecasting (WRF) model used in the study has an architecture that dissolves both the surface and the atmosphere. The high-resolution data can be quickly solved using numerical methods according to the physical options that the user specifies.

Hail event is investigated using WRF atmospheric model. The model domain is set up with 4 nested domains (27, 9, 3 and 1 km resolutions from outer to inner) and Istanbul, located in northwestern Turkey, was used as the central point (41.96°N 20.06°E). Model simulations are performed for 30 hours starting from 18:00 UTC on 26 July 2017, and this time range includes 12-hour spin-up time. The temporal resolution of the outputs obtained for the four domains is 15 minutes for the innermost area and 180 minutes for the outer areas.

In order to be able to construct meteorological conditions real-like, the starting time was determined to be 18 UTC on July 26, 2017. The model was run for 30 hours and the first 6 hours were evaluated as the spin-up time.

ERA-Interim Reanalysis data which has 38 different pressure levels with $0.75^{\circ} \times 0.75^{\circ}$ active and 6-hour temporal resolution was preferred to use as the initial and lateral boundary conditions for the model simulations. In order to compare with the model results, radar, satellite and meteorological station data were taken from Turkish State Meteorological Service.

The performance of the model used in simulating the hail event was assessed by comparing the model outputs and observations. Sensitivity tests were performed for parameterizations such as microphysics, cumulus and boundary layer schemes and different combinations were conducted, because the performance of the model with the default physics options was deemed poor. In the simulations made to predict the hail event, the physics options that can solve the formation of the hail and the vertically developed clouds were investigated. Kain-Fritsch, New SAS, Multi-Scale KF, KF-CuP and New Tiedtke options were used for the cumulus, YSU and MYNN2 options were used for the boundary layer, Dudhia and RRTMG options were used for shortwave radiation, RRTM and RRTMG options were used for long longwave radiation. These parameters were changed for each new simulation and results were analysed for each combination.

The thesis focuses on determining the physics options that improve the performance of WRF model in simulating the hail event. During the process sensitivity tests were performed, reanalysis and observed data were used. Amongst the different combinations, it is found that the model reproduced the hail event fairly well when it is run with Milbrandt 2-moment microphysics scheme, Kain-Fritsch cumulus scheme and MYNN2 planetary boundary layer scheme. Recording to the results, accumulated precipitation is 40 mm from 27 July to 28 July; hail event starts at 14:15 UTC; and the cloud top temperature over Istanbul is about -50 C at the same time. Deep convective clouds reaches about 12 km height. Maximum hail concentration is about 400/kg at 14:15 UTC and it occurs at about 500mb pressure level. Reflectivity is about 50 dBZ when the hail event occurred.

27 TEMMUZ 2017 TARİHİNDE İSTANBUL ÜZERİNDE MEYDANA GELEN DOLU OLAYININ WRF SİMÜLASYONU PERFORMANSI

ÖZET

Dolu gelişimi oldukça bölgesel ve kısa zamanlı bir olay olduğundan dolu yağışı en zor tahmin edilebilen meteorolojik hadiselerdendir. Uzaktan algılama teknolojileri ve kısa süreli tahmin çalışmaları ile takibinin yapılması mümkün olabilmektedir. Yapılan çalışmalarda bilgisayarların artan işlem gücü kapasitesi ve geliştirilen hava tahmin modelleri kullanılmakta, model çıktıları ile gözlemler karşılaştırılarak tahmin yöntemlerinin verimliliği analiz edilmektedir. Meydana gelen hadiseye ve olayın yaşandığı coğrafi bölgeye göre model içerisinde yer alan fizik seçenekleri arasında farklı parametrisasyon kombinasyonları kullanarak meteorolojik hadisenin gerçeğe yakın bir biçimde öngörülebilmesi için benzetimler gerçekleştirilmektedir.

Dolu, dikine gelişimli bulut içerisinde yükselici hava hareketleri sonucu yağışa geçmek isteyen nemli hava içerisinde bulunan damlaların yukarı seviyelere taşınarak sıcaklığı 0°C ile -40°C arasında olan katmanlarda tekrar tekrar donması ve büyümesinin ardından düşüşe geçip buz kütleleri olarak yağışı gerçekleştirmesi olayıdır.

27 Temmuz 2018 tarihinde İstanbul meydana gelen dolu yağışı oldukça şiddetli bir hadise şeklinde yaşanmış, yüzlerce yapı ve binlerce araç zarar görmüştür. İlk olarak saat 12:00 UTC civarında Trakya bölgesinden yurda giriş yapmış, saat 15:00 UTC sıralarında şehrin farklı noktalarında yağmur ve fırtına ile birlikte etkili olmuş ve bu hava olaylarının sonucunda toplamda 30-40 kg yağış kaydedilmiştir.

Kuzey Yarım Kürede orta ve yukarı enlemlerde meydana gelen jetlerin kuvvetlenmesi ve Avrupa üzerinde güçlenen basınç sistemleri sonucunda Trakya bölgesini kapsayan bir alanda yükselici hava hareketleri sonucu dikine gelişimli bulutlar oluşmuş ve bu sistem bir süre bölgede etkili olmuştur. Çalışma alanı olarak dolu yağışının merkezinin olduğu ve ilerlediği alanı içeri alacak şekilde bir bölge belirlenmiştir ve bölgenin merkezinde İstanbul konumlandırılmıştır. Alan bilgileri, başlangıç ve sınır koşulları, veriler ile birlikte modele tanıtılıp dolu benzetimleri yapılmıştır.

Çalışmada kullanılan WRF atmosfer modeli içerisinde hem yüzeyi hem de atmosferi çözüp birleştiren bir mimariye sahiptir. Yüksek çözünürlüklü veriyi kullanıcının belirlediği fiziksel seçeneklere göre sayısal yöntemlerle hızlıca çözebilmektedir.

WRF modelini çalıştırmadan önce iç içe yuvalanmış 4 alan belirlenmiştir. Balkanları ve Türkiye'nin bir kısmını içeren en dış alan 27 km, Marmara Bölgesi'ni ve Trakya'yı kapsayan ikinci alan 9 km, Marmara Bölgesi'nin bir kısmını kapsayan üçüncü alan 3 km ve İstanbul'u içeren dördüncü alan 1 km yatay çözünürlüktedir. Belirlenen dört alan için alınan çıktıların zamansal çözünürlükleri en içeride yuvalanan alan için 15 dakika, dış alanlar için 180 dakikadır.

Hadisenin öngörülebilmesi için yapılan simülasyonlarda dolu yağışının oluşumunu ve dikey gelişimli bulutları çözebilen fizik seçenekleri araştırılmıştır. Mikrofizik için Lin, Milbrant 2-mom ve NSSL 2-mom seçenekleri, kümülüs için Kain-Fritsch, New SAS, Multi Scale KF, KF-CuP ve New Tiedtke seçenekleri, sınır tabaka için YSU ve MYNN2 seçenekleri, kısa dalga radyasyon için Dudhia ve RRTMG seçenekleri, uzun dalga boylu radyasyon için ise RRTM ve RRTMG seçenekleri belirlenmiştir. Her yeni simülasyon için bu parametreler değiştirilerek kombinasyonlar halinde denenmiştir.

Model, meteorolojik koşulların gerçekçi biçimde kurgulayabilmesi için başlangıç saati 26 Temmuz 2017 günü saat 18 UTC olarak belirlenip 30 saat boyunca koşturulmuş ve sonuçlar irdelenirken ilk 6 saat modelin dengeye gelebilmesi için spin-up zamanı olarak kabul edilip 24 saat olarak değerlendirilmiştir.

Modelde kullanılmak üzere $0.75^{\circ} \times 0.75^{\circ}$ alansal ve 6 saat zamansal çözünürlüğe sahip, 38 farklı basınç seviyesi için oluşturulan ERA-Interim Yeniden Analiz verisi tercih edilmiştir. Model sonuçları ile karşılaştırmak üzere Meteoroloji Genel Müdürlüğü'nden dolu olayının yaşandığı tarihlere ait fevk verisi, uydu-radar gözlem verisi, İstanbul'da bulunan meteoroloji istasyonlarından sağlanan ölçüm verileri alınmıştır.

Farklı parametrizasyon kombinasyonları ile yapılan benzetim çıktılarına göre model olay saatine, şiddetine ve merkezine yakın sonuçlar üretmiştir. Model çıktıları ve gözlem verileri bulut tepe sıcaklığı, nemlilik, toplam yağış, dikey hava hareketleri ve yansıma gibi dolu hadisesinin anlaşılmasında önemli rol oynayan hava olaylarının zamanla değişimi karşılaştırılmıştır. Çalışmada şimdiye kadar üretilen en iyi sonuçlardan birini veren kombinasyon NSSL-2-moment mikrofizik seçeneği, Multi-Scale Kain-Fritsch kümülüs seçeneği ve MYNN2 yüzey sınır tabaka seçeneğinin birlikte kullanıldığı parametrizasyon olduğu görülmüştür. Bu seçenekler ile çalıştırılan model çıktısının sonuçları zaman serisi şeklinde, noktasal olarak ve kesit alınarak ayrıntılı şekilde analiz edilmiştir. Buna göre 27 Temmuz 2017 14:15 UTC zamanında bulut tepesi sıcaklığının -50°C , bulut tepesinin yüksekliğinin 12km olduğu görülmüştür. Model sonuçları maksimum dolu miktarını 500mb basınç seviyesinde 400/kg olarak vermiştir. Dolu olayı 50dBZ yansıtıcılık değeri bulunduğu esnada meydana gelmiştir.

1. INTRODUCTION

Hail is frozen form of precipitation that occurs due to unstable air conditions between the surface and middle troposphere. This meteorological event develops in a very short-term and localised manner. Therefore, to predict this meteorological parameter is quite difficult. Generally, hail, which is effective with strong winds and storms, can be dangerous depending on its size and fall speed. On July 27, the heavy hail event damaged hundreds of buildings and thousands of vehicles and it was estimated that the cost of this hazardous event is around 300 Million US Dollars. Understanding the structure and formation of the hail is very important for the prediction of hail events and prevention of disasters.

1.1 Structure and Formation of Hail

The formation of hail requires the deep convective cloud like Cumulonimbus(Cb). Especially in the summer season, daytime boundary layer heating causes the maximum deep convective cloud generation in the afternoon-early evening [1]. At the upper levels, at 20°C - 40°C temperature interval, cloud water droplets which are located within these deep convective clouds become supercooled cloud droplets and then clouds ice crystals [2]. Therefore, the cloud water content is of great importance for the hail growth and suppression [3]. When liquid water content density is used as hail indicator it is understood that water content product could be a useful tool to estimate of hailstorm severity and hail size. The results showed that if liquid water content density is above 3.5 g/m³ then hail diameter is equal to or higher than 19 mm [4]. As a result of ascending and descending air movements, the vertical transport in the cloud is repeated and graupel, one of the hailstorm embryo types, is formed due to the collection of appreciable quantities of supercooled cloud droplets [5]. Besides the vertical movements in the cloud, the severity of these movements is also important. It is demonstrated that the maximum updraft speed should take place in the range 20-40m/s for hail growth. Updrafts of about 50m/s are sufficiently strong to

carry to aloft the embryos without growing. Hail cannot grow in the stronger updraft outside this moderate updraft range [6]. And precipitation in the form of ice has to be at least 5 mm diameter to be defined as hail [7]. Reflectivity factor and cloud top temperature have become quite common techniques for the estimation of hail rate with the advancement of technology and the development of remote sensing methods. Hail size distribution can be characterized by a single parameter radar. The 45 dBZ level is used to define criteria for hail, in the vertical profile of reflectivity [8]. Another technique to strengthen discrimination of hail form is to use the infrared cloud top temperature from the satellite imagery. Depending on reflectivity factor, convective cloud top temperature of -50°C means alert for the possibility of hail event [9]. The occurrence of hailstorm depends on several varieties of meteorologic parameters like temperature, humidity, pressure and wind. Diurnal and seasonal variations affect the formation of hail in connection with these meteorologic parameters. According to research conducted about Turkey's severe hail climatology during 1925-2014, most of the hail events have occurred in May and June between the 12 UTC - 15 UTC [10].

1.2 Literature Review

Hail and extreme precipitation events have negative consequences on the areas where they occur. Therefore, it is very important to define and understand well the processes to predict hail events. The development of measurement, observation methods and remoting sensing technologies, meteorological estimates and atmospheric models have begun to make a greater contribution to the reduction of the risks and harms of such natural disasters. Over the last few years, scientists from different countries of the world have used global or regional climate models that can solve the dynamics between the atmosphere, the ocean and the land using the numerical methods they contain, to predict the meteorological weather events. One of the most used models is the Weather Research and Forecasting (WRF) atmospheric model. WRF atmospheric model contains several physics options like microphysics, cumulus, planetary boundary layer and radiation. These options are changed by the user depending on case study area and weather event under research. Deciding on the options to be used and designing of the model are very important for the consistency of the work. A general literature search has been done to determine the physics options

which we used in this study to simulate hail event. Also, many processes analyzed with WRF that are important for hail formation like cloud condensation nuclei, cyclones, convective movements and ice particles are investigated [11] [12] [13] [14]. The WRF atmospheric model can be operated in a coupled or un-coupled manner with other models. In a study of hail forecasting, the HAILCAST, the One-Dimensional Hail Growth Model, is integrated into the WRF model [15]. The WRF model is widely used in extreme precipitation forecasting and the sensitivity tests of physics options [16] [17] [18]. In one of these studies, the extreme precipitation event on February 20, 2010, in Madeira Island, Portugal is modelled by Dasari and Salgado [19]. The aim of the study was to determine the sensitivity of different microphysical processes on the event. The NCEP FNL analysis data which has 6-hour temporal resolution and the 1x1 spatial resolution is applied as two-way nesting with four different domains with 27, 9, 3 and 1 km horizontal resolution from outer to inner. The WRF model is run on February 19 at 12:00 UTC for 72 hours. For four different microphysical options (Kessler, Lin, Ferrier and Thompson) sensitivity tests were applied. The results are compared with the total rainfall data from observation stations. As a result, it has been decided to diversify the combinations by changing other physics options for better output. Another example of parametrization studies is the WRF performance analysis of the extreme precipitation event in the Ganges basin between 15-18 June 2013 in India, prepared by Chawla et al. [20]. The model has three domains with 27, 9 and 3 km resolution. NCEP FNL analysis data which has 6-hour temporal resolution and the 1X1 spatial resolution is used to run for 121 hours starting from 14 June 00:00 UTC. 4 different microphysical options (Kyon-Fritsch, Betts-Miller-Janjic), 2 different physical planet options (Yonsei University, Mellor-Yamada-Janjic Simple 5-layer Soil Model, Noah) and two different surface models (Lin, Eta, WSM 6, Goddard) were used. The results of the combinations were compared with 18 rainfall gauges and the Tropa Satellite Rainfall Measurement - Analysis (TMPA) data. According to study, the best result is the combination of Goddard microphysics, the Mellor-Yamada-Janjic boundary taka and Betts-Miller-Janjic cumulus alternatives. One of the examples of the simulation of the model of full rainfall is the full storm event of March 9, 2014 in India Baramati, which was worked by Murthy et al. [21]. With the NCEP FNL analysis data, WRF was operated with domain

resolutions of 27, 9, 3, and 1 km for 24 hours from 18:00 UTC on March 20, 2014, then compared with the India Meteorological Department's observational data. Four different microphysical options (Kyon-Fritsch, Betts-Miller-Janjic), 2 different physical planet options (Yonsei University, Mellor-Yamada-Janjic Simple 5-layer Soil Model, Noah) 6, Goddard) were used. As a result of the study, it is stated that more detailed observation is needed for comparison.

1.3 Objectives

Hail event which is occurred on July 27, 2017 is an important event for Istanbul and Turkey. Also, this event is an example of extreme weather events. The structure and formation of the hail phenomenon are studied for many years. The major objectives regarding our study are:

- Understanding the structure of the extreme hail event.
- Performing simulations for the hail event using the atmospheric model.
- Determining parameterizations that give the best simulation of the event.

Another important aim for the future is to understand whether the surface conditions have any effect on the formation, intensification and location of the hail event. Therefore, further sensitivity simulations will be performed.

2. DATA

WRF atmospheric model needs initial and boundary condition to produce weather simulations. Re-Analysis data was used as input to run the atmospheric model and observational data were obtained for the purpose of comparison to the model output.

2.1 Observation Data

Observational data were obtained from Turkish State Meteorological Service (TSMS) for the date of the hail event occurred, during the period between 26 March and 29 March 2017. These are;

- Start time and end time of the hail event for different meteorological stations
- 12-hour rawinsonde and hourly inversion thickness
- 1-minute AWOS data for 32 different stations
- Hourly radar and 15-minute satellite images

2.2 Re-Analysis Data

Air temperature, humidity, wind components and geopotential height fields from ERA-Interim Re-Analysis data set were used to drive the WRF model. the specifications of ERA-Interim data are as follows;

- Spatial Resolution $0,75^{\circ} \times 0,75^{\circ}$
- Temporal Resolution 6 hours
- Time Steps 0000, 0600, 1200, 1800 UTC
- Vertical Resolution 38 level

3. INVESTIGATION OF 7 JULY 2017 HAIL EVENTI

On July 27, 2018, there was an extreme storm in Istanbul. Hundreds of buildings and thousands of vehicles have been damaged. Also, 30-40 kg of precipitation was recorded totally as a result of this weather event. This is an extreme weather event for the geography of Turkey and Istanbul. For this reason, it is very important that the structure of this hail event is well understood and investigated.

3.1 Case Description

Observation data obtained from Turkish State Meteorological Service are investigated. According to satellite and radar observations, when the cloud and rainfall are examined, the system which caused to hail entered the country from Thrace region around 12:00 UTC and hail event influenced different parts of Istanbul with the extreme storm and rainfall events at around 14:15 UTC. Over Istanbul, deep convective clouds occurred and cloud top temperatures were decreased. Weather events which is observed in some stations and their start-end times are given in Table 3.1.

Table 3.1 : Weather event types and times (UTC) of occurrence and station informations

No	Name	Start	End	Event(s)
17060	ATATÜRK AIRPORT	14:20	16:20	Storm, Hurricane
		14:50	19:29	Heavy Rainfall, Flood
		15:03	15:18	Hail
17061	SARIYER	15:25	18:05	Thunderstorm
		16:05	16:08	Hail
17064	KARTAL	15:27	19:00	Heavy Rainfall, Flood
		15:35	15:45	Hail
		18:35	18:45	Hail
17063	SABIHA GÖKÇEN AIRPORT	15:41	19:50	Storm, Hurricane
		15:48	15:50	Hail

According to sudden change report of TSMS, the system that brings the hail is moving towards the east of Istanbul from the west. It is seen that in the event of hail event took

place between 15:03 and 15:18 at Atatürk Airport, while between 15:48 and 15:50 at Sabiha Gökçen Airport. This is a quite fast and short-term event, also system has caused hurricanes, storms and floods. Cloudiness provided by TSMS was given in Figure 3.1. These four satellite images, centred at Istanbul and covered the Marmara region, belong to 13:15, 14:15, 15:15 and 16:15 UTC on July 27, 2017. In the first time step, the system affected the western regions of the Marmara and Thrace region, and then cloudiness and deep of clouds started to increase east of the Marmara region and on the Anatolian side of Istanbul. Referring to clouds found in the inside regions of Turkey, it is clearly seen that the east side of the system is shifting toward the north.

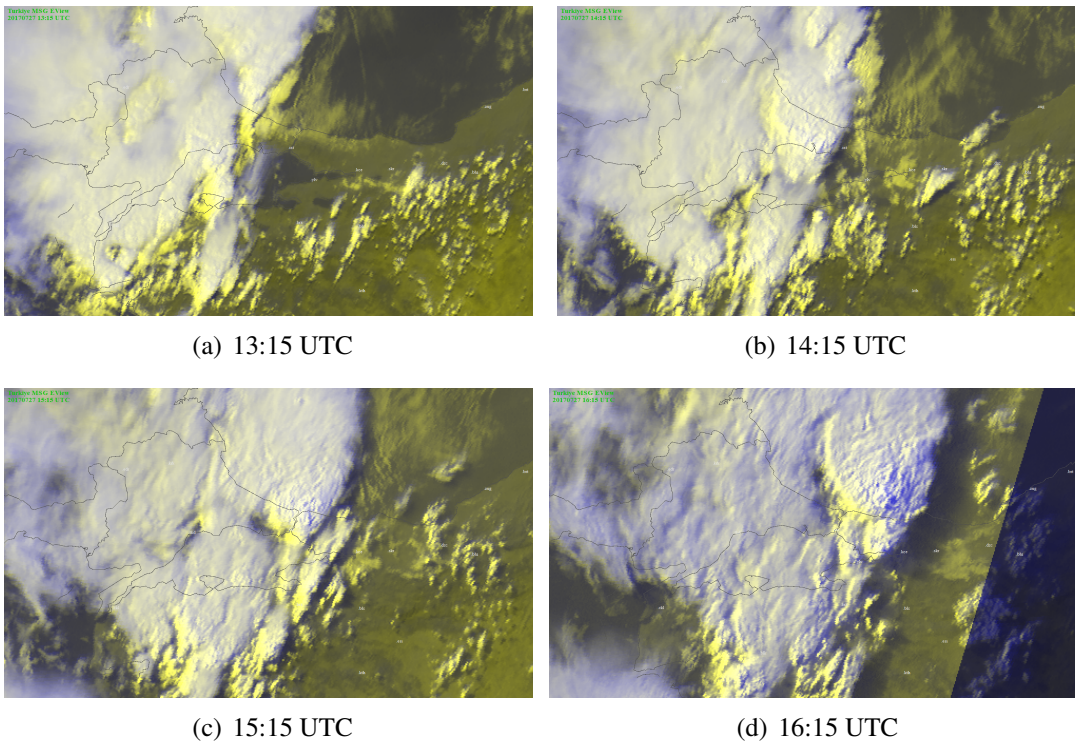


Figure 3.1 : Cloudiness, satellite images on 27.07.2017.

15-minute satellite observation data for cloud top temperature provided by TSMS was given in Figure 3.2. These satellite images, centred at Istanbul and covered the Marmara region, belong to July 27, 2017. The color scale at the bottom left gives the temperature of the cloud top. The red color indicates low cloud top temperatures, while the blue color indicates cloud top temperatures near 0°C. White color shows 0°C, black color shows increasing cloud top temperatures. Low cloud top temperature is interpreted as upper level and deep convective clouds. In the first time step, cloud top temperature is less than zero over the western regions of the Marmara and Thrace region, higher than zero over the Istanbul and east part of Marmara region.

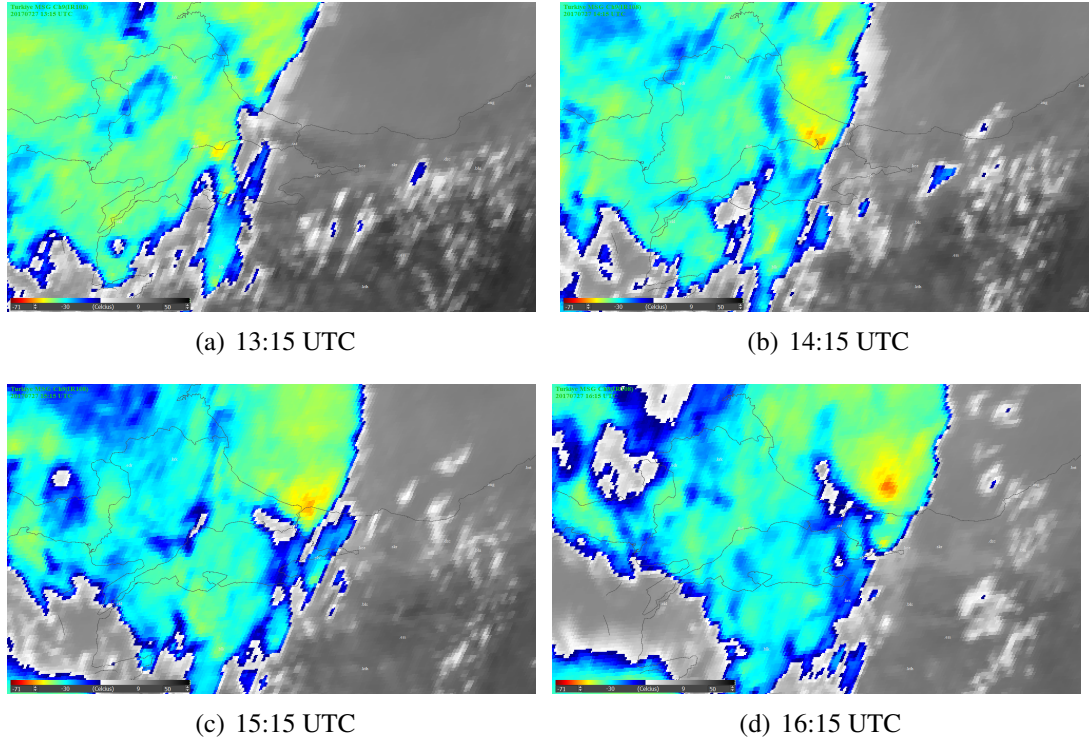
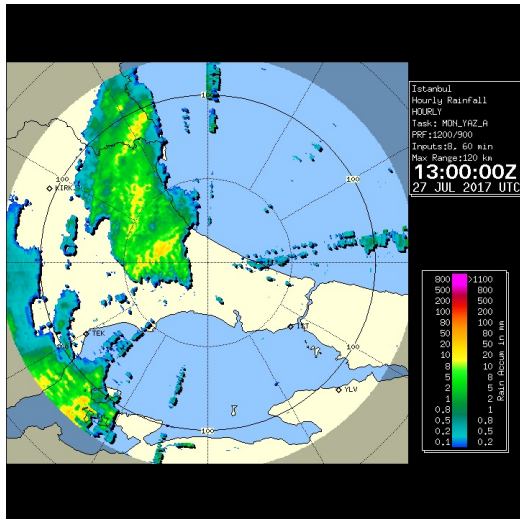


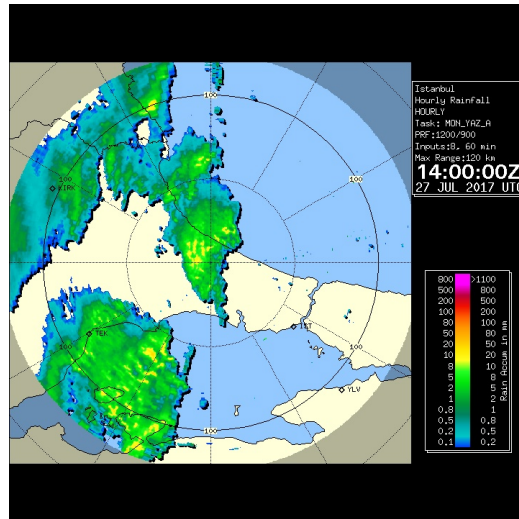
Figure 3.2 : Cloud top temperature, satellite images on 27.07.2017.

Temperatures began to decrease over time. The low cloud top temperature centre on Tekirdağ passed through the Büyükçekmece first, Sarıyer and then moved towards the Black Sea. It is clearly seen that most part of the European side of Istanbul, the cloud top temperatures are less than -15°C at 14:15 UTC. There are also seen that two central points where the cloud top temperatures are around -50°C on Büyükçekmece area. At these points, it is expected that the ascending air movement is strong and the level of the cloud top is high.

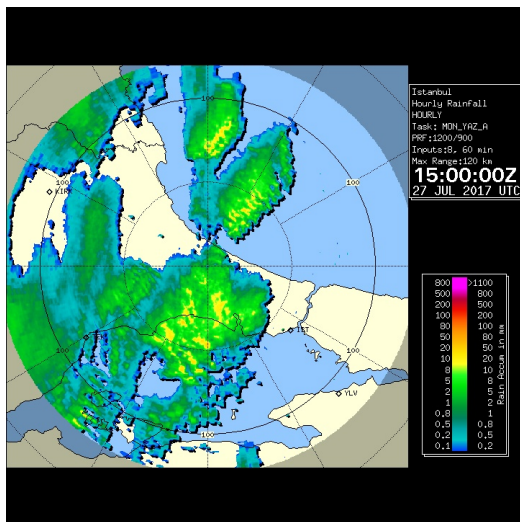
Radar observation data for accumulated provided by TSMS was given in Figure 3.3. These radar images, centred at Istanbul, covered the Marmara region, belong to July 27, 2017 and have 1-hour time resolution. The color scale at the right gives accumulated rain in mm. The hot colors mean excessive rain, while the cold colors indicates low accumulated rain. In the first time step, rain occurred only over the Thrace region. The maximum intense area has about 20mm rain in this time step. Over time, precipitation centers shifted to the north-east and increased their effectiveness. After 14:00 UTC, precipitation occurred over the Istanbul and east part of Marmara region. The rainfall area is increasing over time. The precipitation centre on Silivri



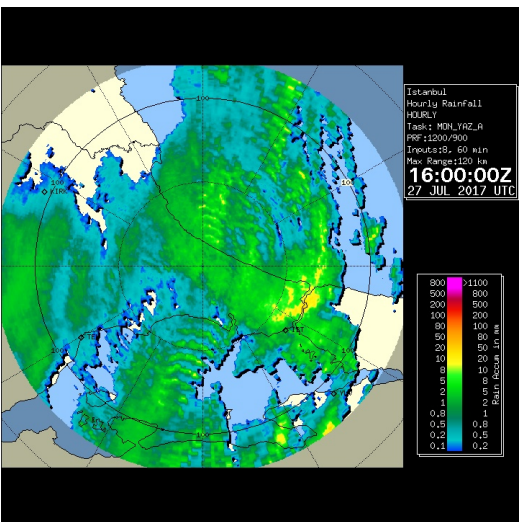
(a) 13:00 UTC



(b) 14:00 UTC



(c) 15:00 UTC



(d) 16:00 UTC

Figure 3.3 : Accumulated rain, 1-hour, radar images on 27.07.2017.

and the Büyükçekmece moved towards the Bosphorus. It is clearly seen that the rainfall is effective almost in the entire Marmara region after 15:00 UTC.

Horizontal winds data belonged to July 27, 2017 provided by TSMS was given in Figure 3.4. These radar images, centred in Istanbul, cover the Marmara region and are obtained at height of 2.5-3.5 km. Each short line in the wind bars indicates 5 knots, each long line indicates the speed of 10 knots and each flag indicates the speed of 50 knots. Also, the empty tails of wind bars indicate the direction in which the wind is going. According to this, it is seen that southern winds are predominant in general. Wind speed is decreasing over time. In the first time step, the speeds of southwesterly winds on the Thrace region are about 20 knots and . Considering wind speeds over the

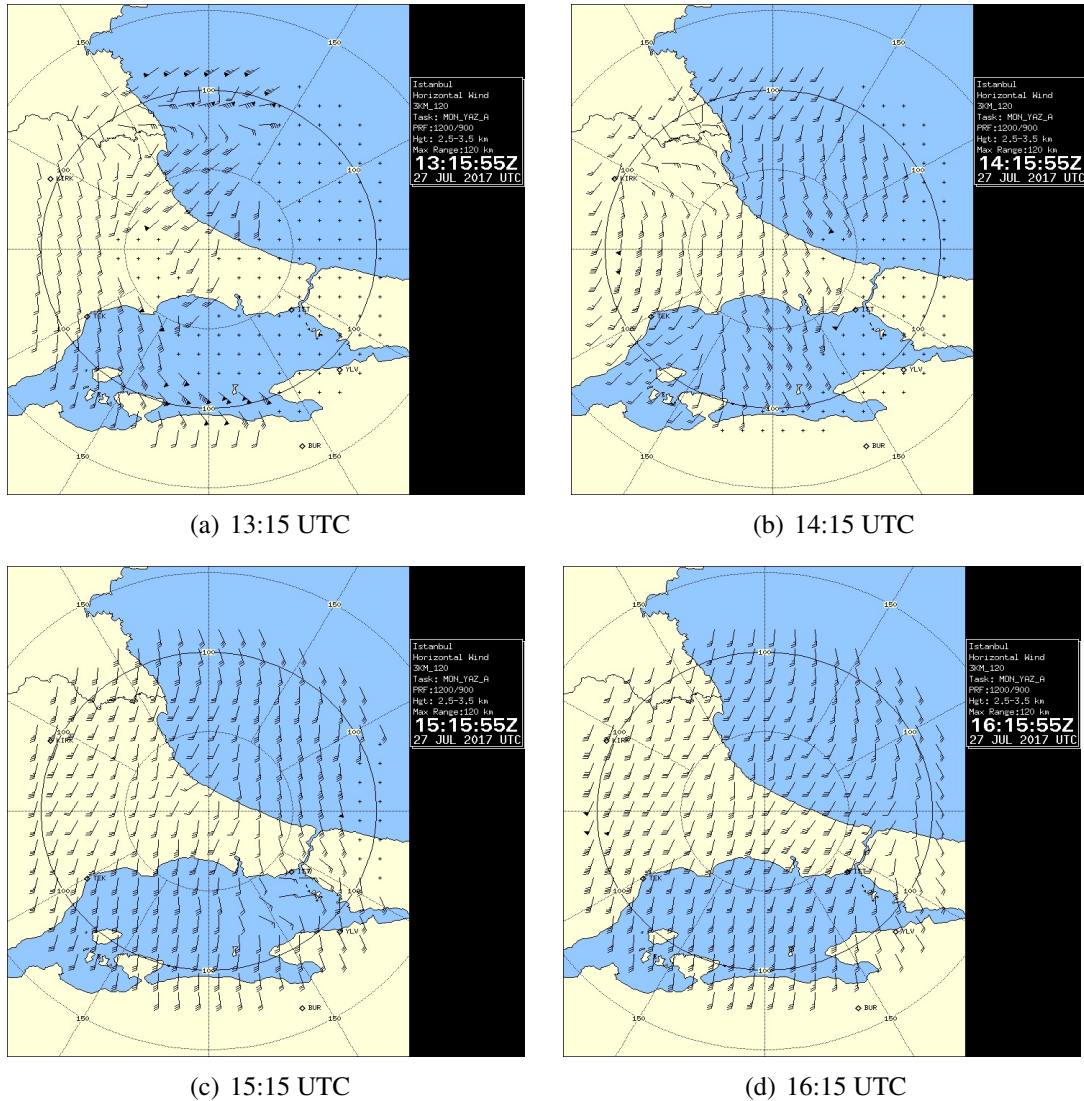
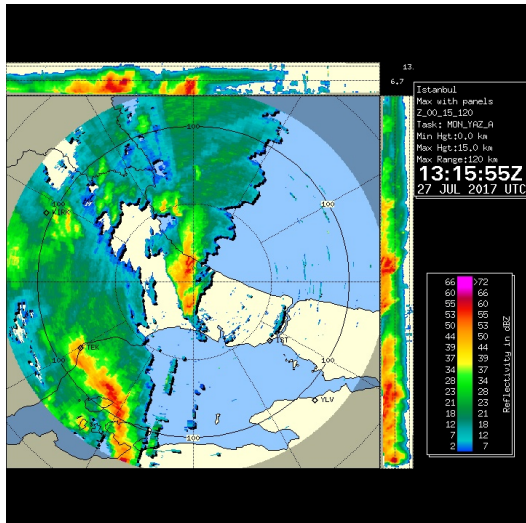


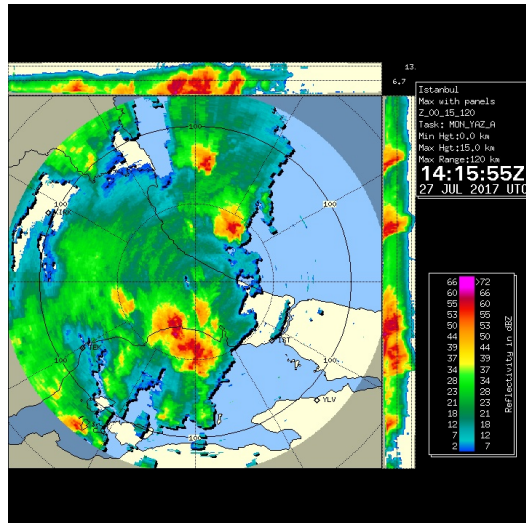
Figure 3.4 : Wind, radar images on 27.07.2017.

Thrace coastline, the winds over the Marmara Sea are faster than wind located on land. On the next time step, southern winds blow from Marmara Sea to Büyükçekmece area with 45 knots.

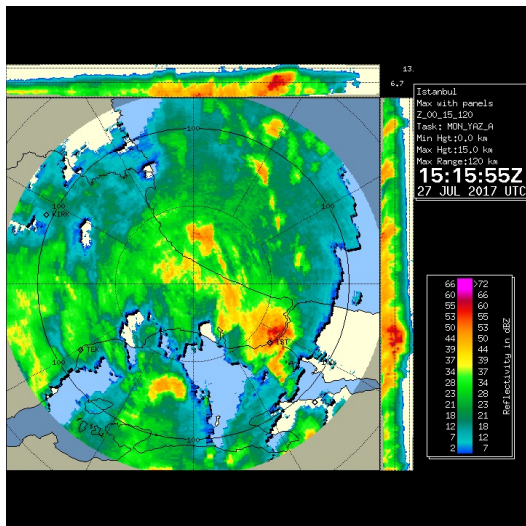
Reflectivity radar observation data provided by TSMS was given in Figure 3.5. These radar images, centred at Istanbul, covered the Marmara region, belong to July 27, 2017 and have 15-minute time resolution. The color scale at the right gives reflectivity in dBZ. The hot colors mean high values, while the cold colors indicates low values about reflectivity. The x and y axes give reflectivity values with altitude for first 13 km height. High reflectivity values are interpreted as high rate of particle concentration found in air and clouds. For instance, when ice particles increase then reflectivity increases. In the first time step, high reflectivity occurred only over the Thrace region.



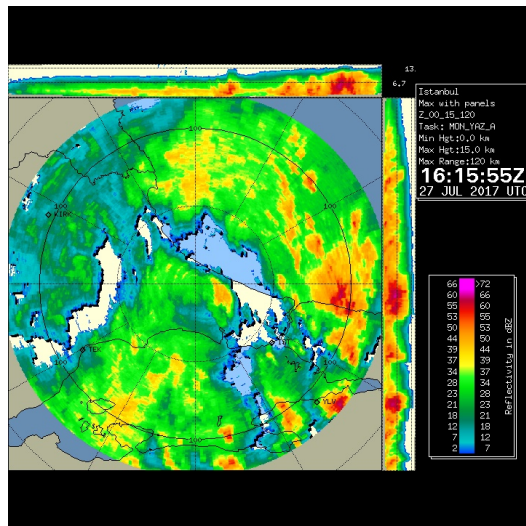
(a) 13:15 UTC



(b) 14:15 UTC



(c) 15:15 UTC



(d) 16:15 UTC

Figure 3.5 : Reflectivity, radar images on 27.07.2017.

The maximum intense area has about 40 dBZ in this time step. Over time, reflectivity centers shifted to the north-east and increased their effectiveness. After 14:15 UTC, reflectivity center located over Silivri and the Büyükçekmece region, moved towards the Bosphorus. It is obvious that, this situation is parallel to precipitation.

Automated Weather Observing System (AWOS) data was obtained from TSMS for 32 different meteorological stations for dates between July 26, 2017, and July 29, 2017. Among them, 11 stations with the least missing data are selected, their names and locations are shown in Figure 3.6 with the terrain height of inner domain. Each AWOS data includes 1-minute average wind direction, average wind speed, maximum wind direction, maximum wind speed, accumulated rain, temperature, relative humidity,

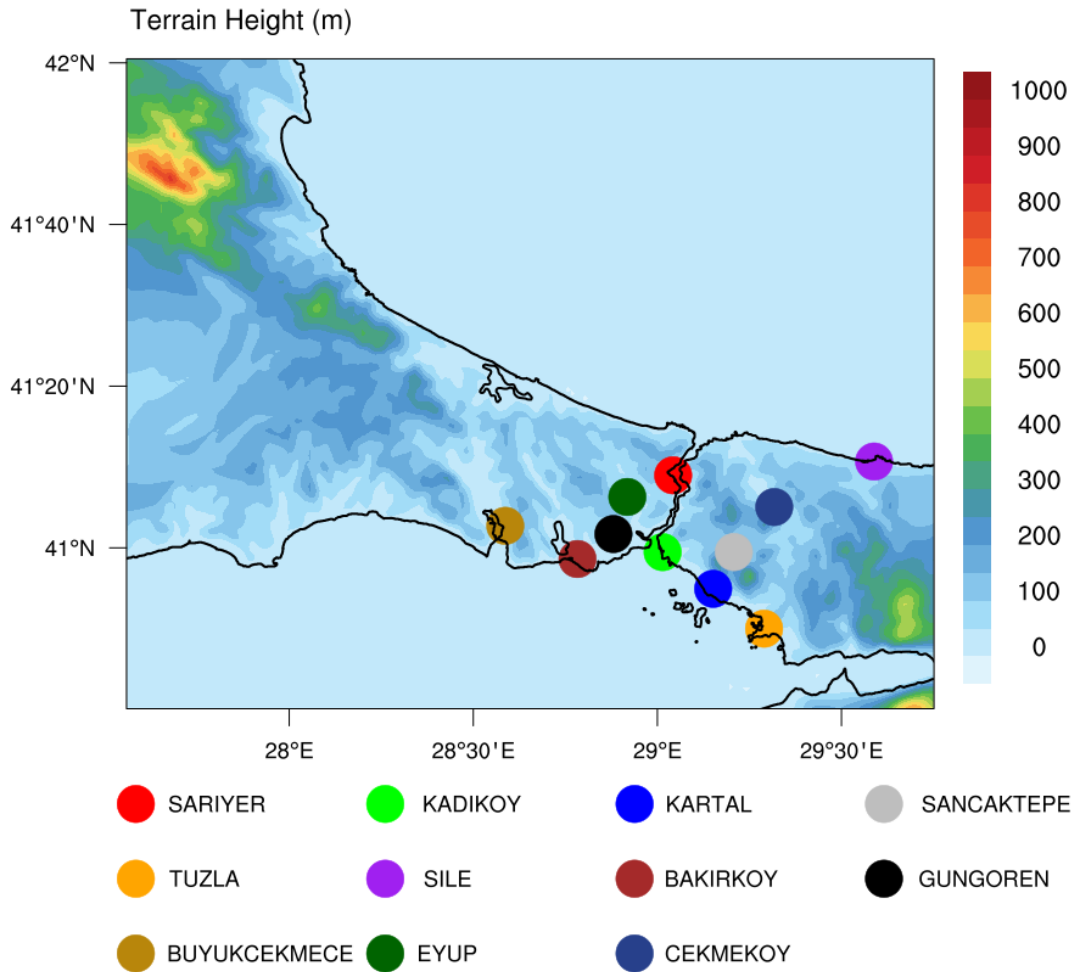


Figure 3.6 : Station names, locations and terrain height of inner domain.

dew point temperature, sea level pressure. In order to understand the hail event, it is necessary to analyze the different time-varying meteorological parameters. For example, at the moment when precipitation occurs, it is also necessary to consider the temperature and the state of the pressure. It is very important that the stations that will be used in the operation contain all of these essential meteorologic parameter values. Meteorological stations that include missing data were identified and were eliminated not to be used in the study. The remaining AWOS data were processed and converted to 15-minute data to compare with model outputs.

15-minute AWOS pressure, temperature, relative humidity and accumulated precipitation data between July 27, 2017, 00:00 UTC and July 28, 2017, 00:00 UTC, is shown in Figure 3.7. In the plot, the x-axis shows the time steps in 15-minute intervals and the y-axis shows the variable and its unit. Each of the colored lines represents a different meteorological station and the names of these stations are given by bottom

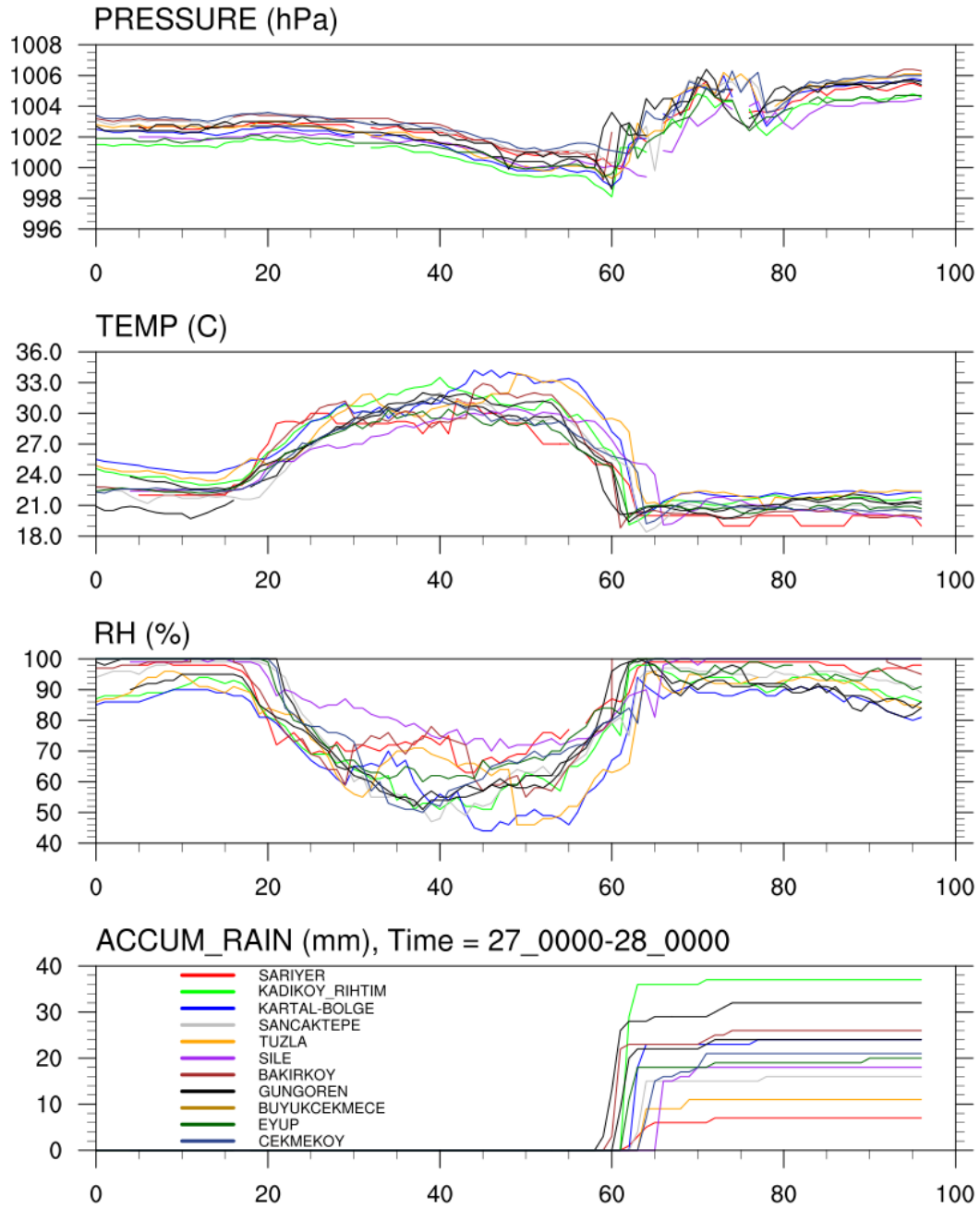


Figure 3.7 : Between 27.07.2017 00:00 UTC and 28.07.2017 00:00 UTC with 15 minutes interval time step, times series for 11 stations.

legend with the line colors. The 60th time step shows 14:15 UTC. When looked at top of the plot, while pressure is decreasing until 998 hPa slightly, it increased suddenly after 14:15 UTC and the measurements became unsteady. At the same time step, the temperature values are also decreasing until 18°C, and not increase too much at following time steps. According to the measuring data, the minimum temperature for some stations is recorded in this time step. Increases and decreases in relative humidity values are measured as the inverse of the temperature values. Relative

humidity reached almost 100% after 14:15 UTC. The accumulated rainfall data from the stations indicate that rain started between 55th and 65th steps, ie between 13:00 UTC and 15:30 UTC. Precipitation was effective within a very short period of time starting at 13:00 UTC and the average amount of rain reached around 20mm. At the end of the day, it is seen that the station with the lowest accumulated precipitation among 11 stations with approximately 10 mm of rain is the Sariyer area indicated by the red line. About 40 mm of rain is observed at the Kadıkoy station indicated by the light green line and the maximum accumulated precipitation occurs at this region.

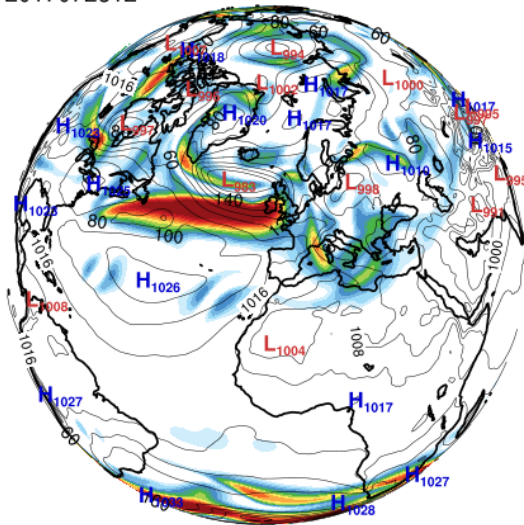
3.2 Synoptic Situation

Synoptic analysis of meteorological situation and examination of general air movements are important for the understanding of case studies. Hail is a very short-term and quite a localised meteorological event. Analyzing of meteorological phenomena like pressure systems, jet streams, vertical velocity and geopotential height at different pressure charts is important for the understanding of the formation of hail event. While some of these meteorological processes can be measured, some are obtained by calculations using basic meteorological parameters such as temperature, pressure and wind. Obtaining, processing and analyzing the observational data in globally are very difficult. Ensemble data that consisted of the model forecast, observation and analysis data is quite useful to calculate and obtain the meteorological parameters in large scale. In this study, the hail event is analyzed synoptically by using the Era-interim reanalysis data.

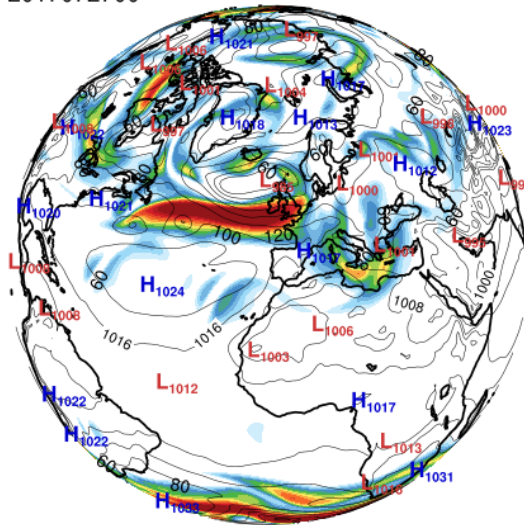
When the reanalysis data are examined, it is seen that a low-pressure center is located over Europe. The upper-level jets influence this low-pressure center. At the same time, over a region that include the Thrace, ascending air movements and deep convective clouds occur.

The ERA-Interim reanalysis data prepared by the European Center for Medium-Range Weather Forecasts (ECMWF) and contained many different meteorological parameters at different pressure levels and surface level. Reanalysis data were obtained from July 26, 2017 to July 29, 2017, for different pressure levels like 850, 500 and 300 hPa for parameters such as geopotential height, relative humidity, temperature, relative vorticity, u and v component of wind.

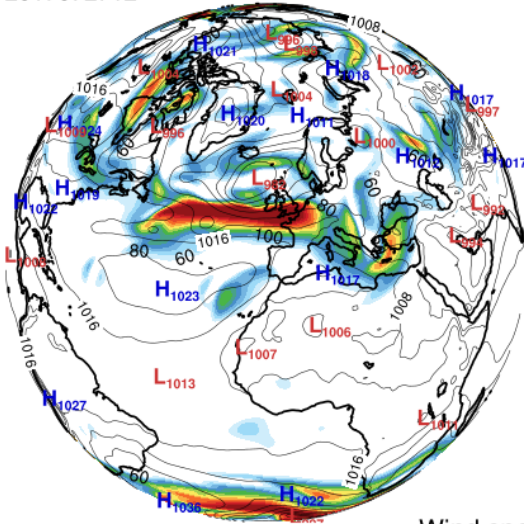
2017072612



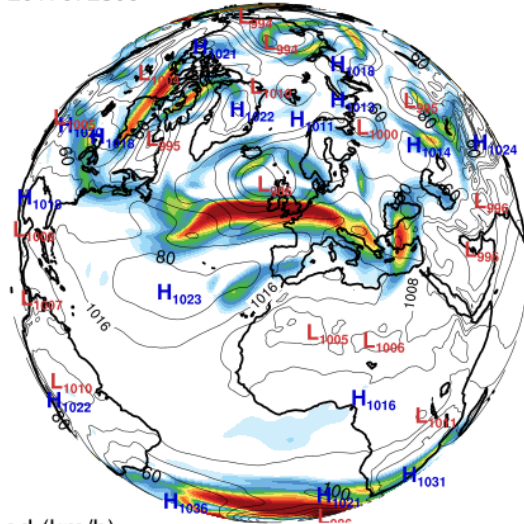
2017072700



2017072712



2017072800



Wind speed (km/h)



Figure 3.8 : Era-Interim, surface pressure (hPa) (4 mb interval contours) and jet stream (km/hour) in 300 hPa pressure level. 26.07.2017 12:00 UTC and 28.07.2017 00:00 UTC with 12-hour time interval.

Some of these meteorological parameters were used in the analysis and Figure 3.8 was prepared for between July 26, 2017, 12:00 UTC and July 28, 2017, 00:00 UTC with 12-hour time interval to examine the upper-level polar jets and pressure areas. The colored areas on the map represent jet winds in km/h, which are effective at the pressure level of 300 hPa. The color scale below the map gives the speed of jet winds. According to scale, the speed of jet winds is increasing from blue to red. The white areas show speeds of 60 km/h or less, the green areas show approximately speed of 120 km/h and the red areas show speeds of 190 km/h and higher. While thin contours show surface level pressure in hPa unit, thick contours show land boundaries. Pressure

contours were plotted at intervals of 4 hPa from 992 to 1024. The letter H in blue indicates the high pressure center, and the letter L in red indicates the low pressure center. The numbers at the bottom right of the capital letters indicate the pressure value in hPa unit of that pressure center. The map was plotted for the northern hemisphere and centered on the North Atlantic Ocean. Accordingly, Turkey is located on the right side of the plotted world map. In the first time step, high pressure center is located over the North Atlantic Ocean with a value of 1026 hPa, which effect large area near the equator. There is also another high pressure center located in the southeast of Canada. The "Icelandic Low" is over the North Atlantic Ocean near the north pole and another low pressure is centered is over Europe. The low pressure center is called the cyclone and the high pressure center is called the anticyclone. Convergence occurs on the surface that is dominated by the cyclones, and divergence occurs on the surface that is dominated by the anticyclones. In the northern hemisphere because of the effect of the Coriolis force, the air movement is formed anti-clockwise over the cyclones, while clockwise over the anticyclones. Therefore, the jets seen in the northern half-sphere move from west to east. Over the North Atlantic Ocean, a jet stream with winds at 190 km/h and higher starting from the east of Canada to the western part of Europe, is seen. In the next time step, the low center is moved to Europe, where it encounter another low pressure center over Northern Europe. Jet winds likewise have moved up to the inner part of Europe and winds with speeds of 150 km/h have blowed through Turkey by circumventing the low pressure. As time progresses, the winds approached Europe and became more effective in inner regions.

Geopotential height and winds at 500 hPa pressure level were plotted for the same time steps by using ERA-Interim reanalysis data [Figure 3.10]. The numbers on the border of the map show the latitude and longitude values of the area determined for the plotting. According to this, the map is located between 30 and 70 North latitudes, between 60 West and 50 East longitudes. The colored areas on the map represent geopotential height in gpdam. According to scale, the values of relative vorticity are increasing from cold colors to warm colors. Arrows in this pressure chart mean wind speed and direction. Length of reference vector which is 30 km/h were used for specified other arrows value. The map was drawn to include Turkey, Europe and the north part of North Atlantic Ocean. Turkey is located at the bottom right

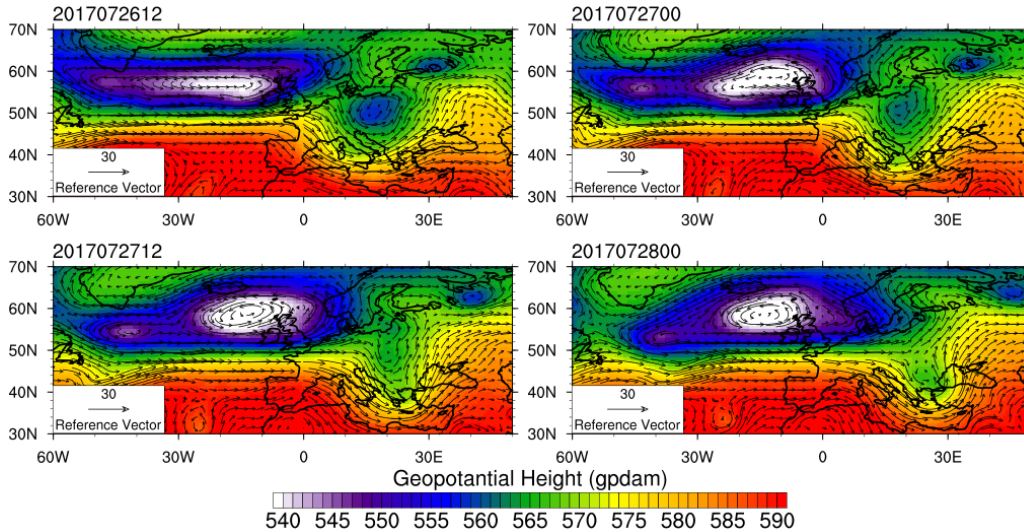


Figure 3.9 : Era-Interim, geopotential height (gpdam) and winds (km/h) in 500 hPa. 26.07.2017 12:00 UTC and 28.07.2017 00:00 UTC with 12-hour time interval.

of the map. In the first time step, it is seen that a large area just below Iceland has very low geopotential height values. Other low geopotential height center is located over Europe. Over the North Atlantic Sea, the strong winds that flow from the east of Canada to Europe, reaches Turkey cross under of this center. As time passes, center on Europe extends onto the near of Turkey and the winds are accelerated even further. Geopotential height shows the actual height of a pressure surface above mean sea-level. Cold air is more dense than warm air. It causes pressure surfaces to be lower in colder air masses. So, geopotential heights are lower in cold air masses and height values reduced from 590 gpdam to 570 gpdam over Marmara region at July 27, 2017, 12:00 UTC.

Relative vorticity and winds at 300 hPa pressure level and mean sea level pressure were plotted for the same time steps by using ERA-Interim reanalysis data [Figure 3.10]. The numbers on the border of the map show the latitude and longitude values of the area determined for the plotting. According to this, the map is located between 30 and 62 North latitudes, between 175 West and 50 East longitudes. The colored areas on the map represent relative vorticity in $10E-5/s$. The color scale below the map gives the values of relative vorticity. According to scale, the values of relative vorticity are increasing from blue to red. The blue areas show speeds of $-18 10E-5/s$ or less, the green areas show approximately speed of $6 10E-5/s$ and the red areas show speeds of $36 10E-5/s$ and higher. While white contours show mean surface level pressure in hPa

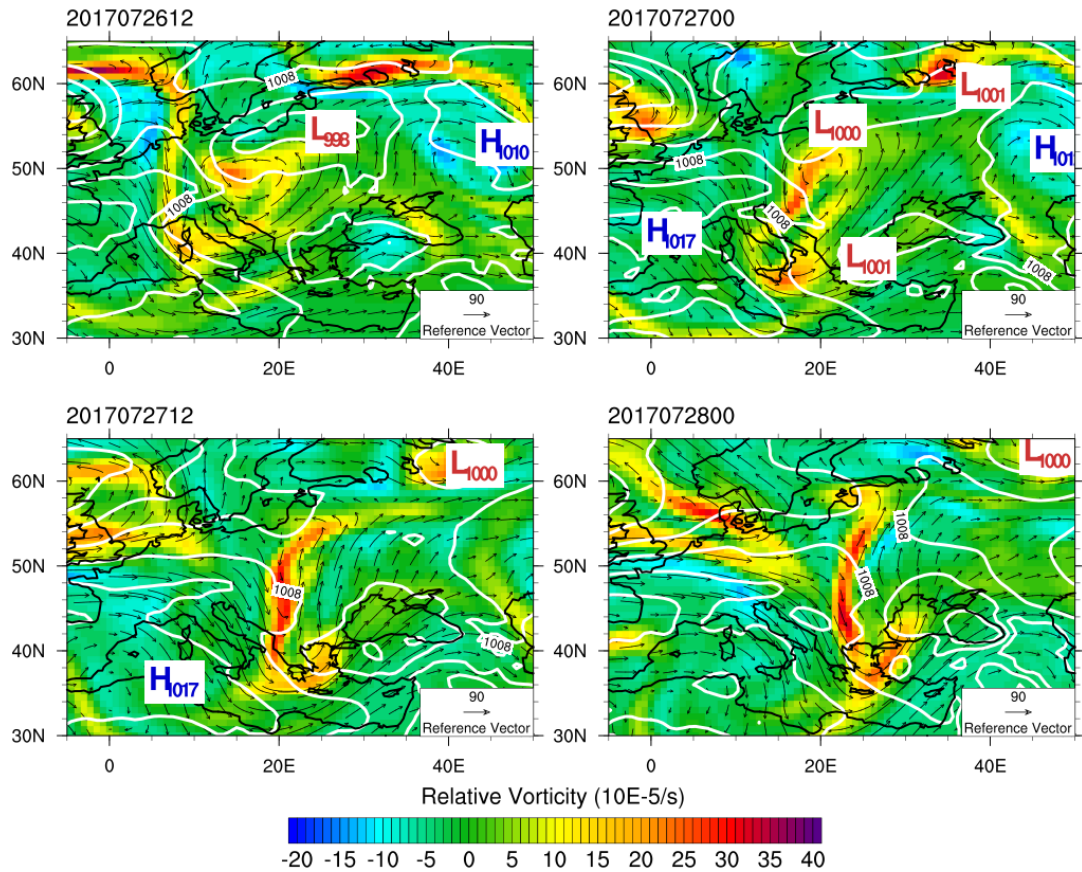


Figure 3.10 : Era-Interim, mean sea level pressure (hPa) (4 mb interval contours) and relative vorticity ($10E-5/s$) in 300 hPa. 26.07.2017 12:00 UTC and 28.07.2017 00:00 UTC with 12-hour time interval.

unit, black contours show land boundaries. Pressure contours were plotted at intervals of 4 hPa from 992 to 1024. The letter H in blue indicates the high pressure center, and the letter L in red indicates the low pressure center. The numbers at the bottom right of the capital letters indicate the pressure value in hPa unit of that pressure center. Arrows in this pressure chart mean wind speed and direction. Length of reference vector which is 90 km/h were used for specified other arrows value. The map was drawn to include Turkey and the most part of Europe. Turkey is located at the bottom right of the map. The red areas indicate that there are ascending air movements and blue areas indicate descending air movements. It is seen that in the third and fourth steps there are strong northeasterly winds over the European area, southeasterly winds over Turkey, and strong ascending air movements over the western part of Turkey. According to the map plotted for July 27, 2017, 12:00 UTC, the relative vorticity value over the Marmara Region is about $20 \cdot 10E-5/s$, the pressure value is between 1000 and 1004 hPa and the wind speed is about 120 km/h.

4. MODEL

In the studies related to weather prediction and synoptic analysis, high performance computers and improved weather forecasting models are used. The efficiency of prediction methods were analyzed by comparing the observation with model outputs. In this study, simulations have been obtained for the purpose of predicting the meteorological phenomenon most close to reality by changing the physics options of the model. The Weather Research and Forecasting (WRF) atmospheric model was used for this purpose.

4.1 The WRF Model

The Weather Research and Forecasting (WRF) Model is a state-of-the-art numerical weather prediction system designed for both research and forecasting applications. National Center for Atmospheric Research (NCAR) started to develop WRF that offers a flexible and computationally-efficient platform while reflecting recent advances in physics, numerics, and data assimilation.

The WRF system contains two dynamical solvers, referred to as the ARW (Advanced Research WRF) core and the NMM (Nonhydrostatic Mesoscale Model) core. The ARW dynamics solver works with other components of the WRF to produce a simulation. WRF consists of physics schemes, numerics/dynamics options, initialization routines, and a data assimilation package. ARW is a subset of the WRF modelling system.

4.2 Model Setup

It was considered that the model would be operated most efficiently and cheaply during model installation. According to this, the model domain is set up with 4 nested domains (27, 9, 3 and 1 km resolutions from outer to inner) and Istanbul, located in northwestern Turkey, was used as the central point (41.96°N 20.06°E). Model simulations are performed for 30 hours starting from 18:00 UTC on 26 July

2017, and this time range includes 12-hour spin-up time. The temporal resolution of the outputs obtained for the four domains is 15 minutes for the innermost area and 180 minutes for the outer areas.

4.2.1 Study area

The study area was determined by taking into consideration the regions where the meteorological event was developed and affected. The designated study area and domains to be processed in the WRF Preprocessing System (WPS) are shown in the Figure 4.1. Each of the nested frames represents a domain. The numbers on the border of the map show the latitude and longitude values of the area determined for the studying. According to this, the outer domain is located between 38 and 46 North latitudes, between 23 and 33 East longitudes. The second domain is located between 39 and 44 North latitudes, between 25 and 31 East longitudes. The third domain is located between 40 and 43 North latitudes, between 26 and 30 East longitudes. The inner domain is located between 41 and 42 North latitudes, between 27 and 29 East longitudes. The colored areas on the map represent terrain height in meters. The color scale on the right side of the map gives the values of the terrain height. According to scale, the values of terrain height are increasing from green to yellow. The light green areas show the height of 0 m, in other word, the mean sea level, and the yellow areas show the height of 3000 m and higher. Black contours show land boundaries. The surface data show that there are surface features of about 3000 meters in the Balkans and in the region of the Thrace. The maximum altitude in the topography of Istanbul is about 500 m. The model performs all operations only on these specified domains. WPS geographical input data sets are used when generating terrestrial data during WPS step. Ready terrestrial data set is presented within the model itself. Moderate Resolution Imaging Spectroradiometer (MODIS) prepared by The Global Land Cover Facility (GLCF) was used as the geographical data set. The terrestrial properties of the surface in which the domains are located are prepared as WRF input. The terrain height data which is available in the model output was used to plot domains.

The horizontal resolution of the MODIS data is $0.5^{\circ} \times 05^{\circ}$. MODIS-based data contains 21 categories of land use like croplands, urban and built-up, snow and ice, mixed forests. The grid resolution specified for domains during the model simulation is a

significant factor for output. Higher resolution data means more frequent numerical calculation, hence there occur fewer errors. The model that run with input data with low resolution gives a poor output. On the other hand, high-resolution data processing takes a long time and consumes a lot of computer power. Therefore, it is important to make optimum choices about resolution. While the input data must be of a high resolution enough to resolve the meteorological process well, the simulation cost should be kept low. Thus, in the study, the surface resolutions of the first three domains covering the largest area are 27 km, 9 km and 3 km respectively. The horizontal resolution of the innermost domain is 1 km. In the figure where the study area is shown, the resolution difference between of the domains caused the color mismatches at the nesting borders. On the map, the black and white parts on the left side of the outer domain are due to differences of the map projections.

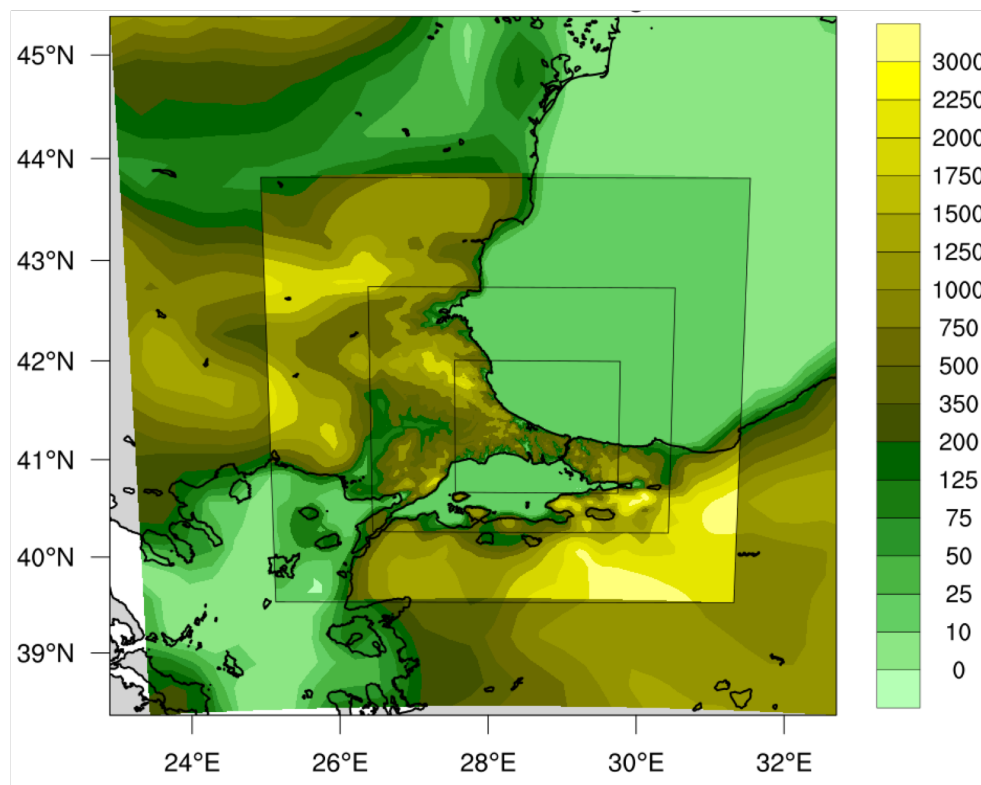


Figure 4.1 : Domains and terrain (m).

4.2.2 The physics schemes

The physics options were determined by taking into consideration the kind of meteorological event. Physics options are quite effective on model outputs. The physics options to be used in the study are as follows;

- Microphysics; Lin [22], Milbrandt 2-mom [23] [24], Goddard [25], NSSL 2-mom [26]
- Cumulus; Kain Fritsch [27], New SAS [28], Multi Scale KF [29], KF-Cup [30], New Tiedtke [31]
- Planetary Boundary Layer; YSU [32], MYNN2 [33] [34]
- Short-wave Radiation; Dudhia [35], RRTMG [36]
- Long-wave Radiation; RRTM [37], RRTMG [36]

Other model settings, such as physics options, are also effective on model outputs. During the study, we tried to determine the values that gave the best results among other physics options, like minutes between radiation physics calls, number of vertical levels and minutes between cumulus physics calls.

4.3 Post-Processing

Making the outputs meaningful is very important for the analysis. After the model is run, the model outputs are post-processed for the purpose. Outputs have been visualized as two-dimensional and three-dimensional using corresponding software and programs.

5. RESULTS

The model outputs are firstly compared with the observation data and the best parametrization configuration was determined. Then, the combination of physics options that best simulate the meteorological event is explained and the results of this model are analyzed in detail.

5.1 Performance of the Model

The WRF model contains predefined variables. These variables are rearranged by the user according to the model output and speciality of the weather event to be worked on. These options have been tested separately to see how they affect results. Combinations of these options were given at Table 5.1 for each experiment. Every different microphysical options were compared by running the model. Options considered to be better are kept constant.

Different spin-up times are used in this study. 25th July 00:00 UTC, 26th July 00:00, 12:00, 18:00 UTC and 27th July 00:00 UTC are used as initial time of run. The spin-up time was decided to be 6 hours. Sensitivity simulations conducted with Lin, Milbrandt 2-mom, Goddard and NSSL 2-mom schemes microphysics options, and New SAS, Multi Scale KF, Kain Fritsch KF-Cup and New Tiedtke schemes cumulus options. YSU and MYNN2 schemes for PBL options, and for Dudhia and RRTMG schemes short-wave radiation options and for RRTM and RRTMG schemes long-wave radiation options were performed to evaluate the microphysics parameterization effect for the case study. Different input data with a pressure level of 28 and 38 are used and the value of "lvl" is changed accordingly. The study has been continued with input data having 38 different levels. 41 and 28 levels are used for the vertical resolution of model output. It was observed that the outputs were more successful when using 41 levels. Surface layer physics parameter is based on PBL option. When used with YSU, surface layer option is 1, while when used with MYNN2 it can be 1, 2 and 5.

Table 5.1 : Experiment numbers and options

No	Init Time	Microphysics	Cumulus	PBL	Sw Rad	Lw Rad	lvl	evert	sfclay	tstep	cutd
1	1800-26	Lin	Kain-Fritsch	YSU	Dudhia	RRTM	38	28	1	162	5
2	1800-26	Milbrant 2-mom	Kain-Fritsch	YSU	Dudhia	RRTM	38	28	1	162	5
3	1800-26	NSSL 2-mom	Kain-Fritsch	YSU	Dudhia	RRTM	38	28	1	162	5
4	1800-26	NSSL 2-mom	Kain-Fritsch	YSU	Dudhia	RRTM	28	28	1	162	5
5	1800-26	NSSL 2-mom	New SAS	YSU	Dudhia	RRTM	28	28	1	162	5
6	1800-26	NSSL 2-mom	New SAS	YSU	Dudhia	RRTM	38	28	1	162	5
7	1800-26	NSSL 2-mom	Multi Scale KF	YSU	Dudhia	RRTM	28	28	1	162	5
8	1800-26	NSSL 2-mom	Multi Scale KF	YSU	Dudhia	RRTM	38	28	1	162	5
9	0000-26	Milbrant 2-mom	Kain-Fritsch	YSU	Dudhia	RRTM	28	28	1	162	5
10	0000-27	Milbrant 2-mom	Kain-Fritsch	YSU	Dudhia	RRTM	28	28	1	162	5
11	1200-26	Milbrant 2-mom	Kain-Fritsch	YSU	Dudhia	RRTM	28	28	1	162	5
12	1800-26	Milbrant 2-mom	Kain-Fritsch	YSU	Dudhia	RRTM	28	28	1	162	5
13	1800-26	Milbrant 2-mom	Kain-Fritsch	YSU	Dudhia	RRTM	38	28	1	162	5
14	1800-26	Goddard	Kain-Fritsch	YSU	Dudhia	RRTM	38	28	1	162	5
15	0000-25	Milbrant 2-mom	Kain-Fritsch	YSU	Dudhia	RRTM	38	28	1	162	5
16	1800-26	NSSL 2-mom	KF-CuP	YSU	Dudhia	RRTM	38	28	1	162	5
17	1800-26	NSSL 2-mom	New Tiedtke	YSU	Dudhia	RRTM	38	28	1	162	5
18	1800-26	Milbrant 2-mom	Multi Scale KF	YSU	Dudhia	RRTM	38	28	1	162	5
19	1800-26	Milbrant 2-mom	Multi Scale KF	YSU	RRTMG	RRTMG	38	28	1	162	5
20	1800-26	Milbrant 2-mom	Multi Scale KF	YSU	RRTMG	RRTMG	38	28	1	162	0
21	1800-26	Milbrant 2-mom	Kain-Fritsch	YSU	Dudhia	RRTM	38	41	1	162	5
22	1800-26	Milbrant 2-mom	Kain-Fritsch	MYNN2	Dudhia	RRTM	38	41	1	162	5
23	1800-26	Milbrant 2-mom	Kain-Fritsch	MYNN2	Dudhia	RRTM	38	41	5	162	5
24	1800-26	NSSL 2-mom	Kain-Fritsch	MYNN2	Dudhia	RRTM	38	41	5	150	5
25	1800-26	NSSL 2-mom	Kain-Fritsch	MYNN2	Dudhia	RRTM	38	41	5	162	5
26	1800-26	Milbrant 2-mom	Kain-Fritsch	MYNN2	Dudhia	RRTM	38	41	5	100	5
27	1800-26	Milbrant 2-mom	Kain-Fritsch	MYNN2	Dudhia	RRTM	38	41	5	150	5
28	1800-26	Milbrant 2-mom	Kain-Fritsch	MYNN2	Dudhia	RRTM	38	41	5	180	5
29	1800-26	Milbrant 2-mom	Kain-Fritsch	MYNN2	RRTMG	RRTMG	38	41	5	162	5

Time step is related to the integration of data and depends on the specified temporal resolution of model output and horizontal resolution of the domain. 150,162 and 180 seconds are used as a time step, respectively, and no significant difference was observed. "cudt" means minutes between cumulus physics call and its default value is 5. A value of 0 is tried but no change has been observed.

5.1.1 Sensitivity study with different microphysics schemes

Four different microphysical options were identified in the study: Lin, Milbrandt 2-mom, Goddard and NSSL 2-mom. All physical options of the model were held steady and the model was run again for six different microphysics options. Model outputs were compared in itself for each microphysics option. In this way, it was aimed to determine the microphysics scheme which gave the best simulate of the hail event. other physics options are given with Table 5.2. Kain-Fritsch, YSU, Dudhia, RRTM, 38, 28, 1 162, 5 and 30 are used as cumulus, PBL, shortwave radiation and longwave radiation physics scheme, number of incoming vertical levels, eta levels, surface layer, time step, minutes between cumulus physics call and minutes between cumulus physics, respectively.

Table 5.2 : Experiments and specified options for microphysics comparing

No	Microphysics	Cumulus	PBL	Sw Rad	Lw Rad
1	Lin	Kain-Fritsch	YSU	Dudhia	RRTM
3	NSSL 2-mom	Kain-Fritsch	YSU	Dudhia	RRTM
13	Milbrant 2-mom	Kain-Fritsch	YSU	Dudhia	RRTM
14	Goddard	Kain-Fritsch	YSU	Dudhia	RRTM

Model outputs which run using four different microphysical options were compared for cloud top temperatures, hail and accumulated rain at 27 July 2017 14:15 UTC in Figure 5.1. In comparison, options were kept constant except for microphysics option. The microphysics options that the maps belong to are written on plots. The numbers on the border of the map show the latitude and longitude values of the area determined for the plotting. According to this, the map centred on Istanbul and included some part of Thrace region is located approximately between 40 and 42 North latitudes, between 27 and 30 East longitudes. Thick and black contours show land boundaries.

At the first part, the coloured areas show cloud top temperature in °C. The colour scale on the right side of the map gives the temperature of the cloud top. The red

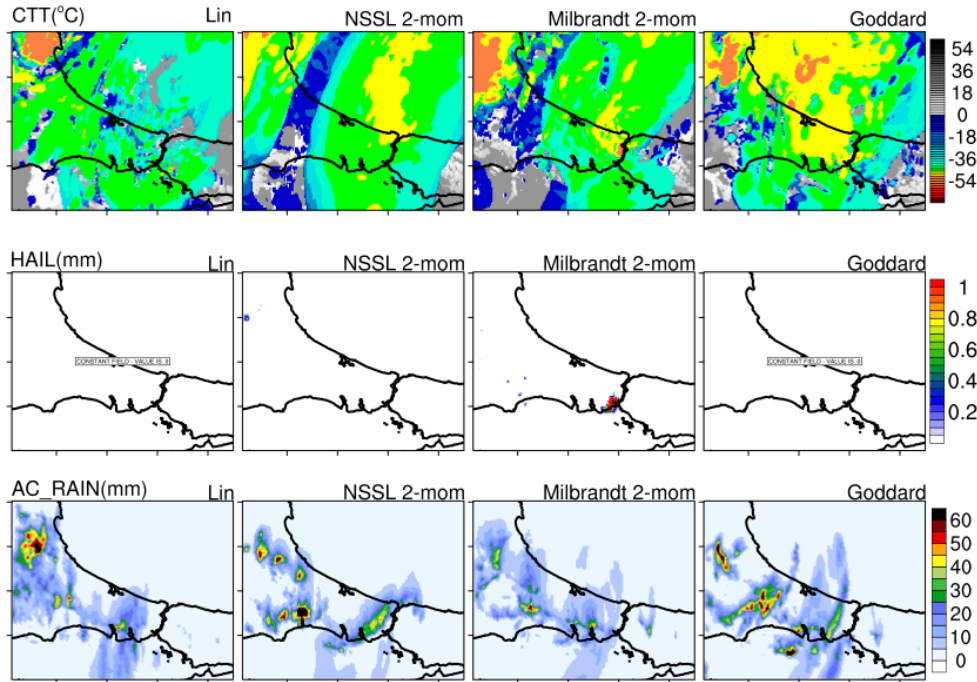


Figure 5.1 : Cloud top temperature($^{\circ}\text{C}$), hail(mm) and accumulated rain(mm) for microphysics schemes on July 27, 2017 at 14:15 UTC.

colour indicates cloud top temperatures of -70°C or colder, while the blue colour indicates cloud top temperatures near 0°C . White colour shows 0°C temperature, black colour indicates cloud top temperatures of 70°C or warmer. The map obtained from the outputs of the model run by Lin microphysics option shows that the cloud top temperatures have decreased to as low as -60°C in north of Thrace region. The cloudiness in the other regions seems rather scattered and the temperature is around -40°C . At NSSL map, it is seen that cloud top temperature over Büyükçekmece coastline area of the Marmara Sea, and Black Sea side of Bosphorus are around -50°C . In the Milbrandt map, cloud top temperature about -55°C is located on the Bosphorus as a center. A big part of the European side of Istanbul is about -50°C according to Goddard scheme.

The second part shows hail in millimeter. The colour scale on the right side of the map gives the amount of the hail. While the white colour shows areas where the total amount of hail is 0.1 mm or less, the black colour shows areas where the total amount of hail is 1 mm or more. Lin and Goddard did not produce any hail as output data. Nssl produced very few hail for Thrace area. According to the map obtained from the output of the model working with Milbrandt 2-mom microphysical option, in a small area of Bosphorus region, 0.9 mm hail was observed.

In the third and last part, the coloured areas show shows accumulated rain in millimeter. The colour scale on the right side of the map gives the amount of the rain. While the white colour shows areas without rainfall, the black colour shows areas where the total amount of accumulated rain is 60 mm or more. Lin and Milbrandt gave rainfall event for the Thrace region and the European side of Istanbul. 40 mm precipitation is seen around Büyükçekmece and Küçükçekmece for these maps. NSSL and Goddard gave rainfall events especially for the European side near the Bosphorus.

5.1.2 Sensitivity study with different cumulus schemes

Five different cumulus options were identified in the study, Kain Fritsch, New SAS, Multi Scale KF, KF-Cup and New Tiedtke. All physical options of the model were held steady and the model was run again for four different cumulus options. Model outputs were compared in itself for each cumulus option. In this way, it was aimed to determine the microphysics scheme which gave the best simulate of the hail event. other physics options are given with Table 5.3. NSSL 2mom, YSU, Dudhia, RRTM, 38, 28, 1 162, 5 and 30 are used as microphysics, PBL, shortwave radiation and longwave radiation physics scheme, number of incoming vertical levels, eta levels, surface layer, time step, minutes between cumulus physics call and minutes between cumulus physics, respectively.

Table 5.3 : Experiment numbers and options for cumulus

No	Microphysics	Cumulus	PBL	Sw Rad	Lw Rad
3	NSSL 2-mom	Kain-Fritsch	YSU	Dudhia	RRTM
6	NSSL 2-mom	New SAS	YSU	Dudhia	RRTM
8	NSSL 2-mom	Multi Scale KF	YSU	Dudhia	RRTM
16	NSSL 2-mom	KF-CuP	YSU	Dudhia	RRTM
17	NSSL 2-mom	New Tiedtke	YSU	Dudhia	RRTM

Model outputs which run using five different cumulus options were compared in the same way in Figure 5.2. In comparison, options were kept constant except for cumulus option. The cumulus options that the maps belong to are written on plots.

If we look at the map showing cloud top temperature, the outputs of the model run by KF only shows that the cloud top temperatures have decreased to as low as -50°C over the north of Bosphorus, while MS-KF and KF-CuP cumulus options show that the cloud top temperatures have decreased to as low as -50°C also over the European side of Istanbul. According to the model run with New SAS, almost the whole map

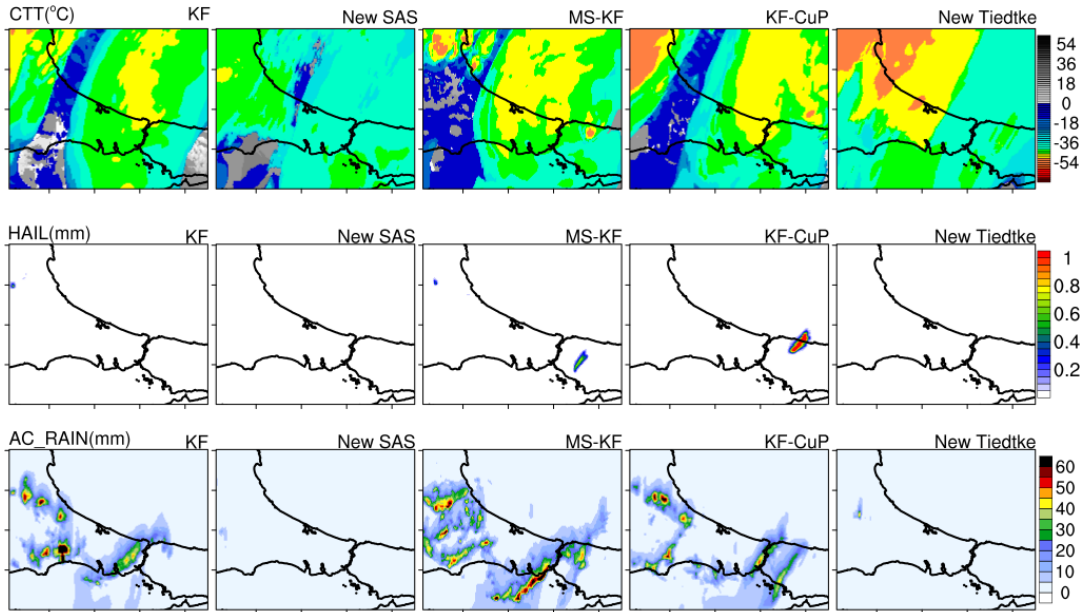


Figure 5.2 : Cloud top temperature($^{\circ}$ C), hail(mm) and accumulated rain(mm) for cumulus schemes on July 27, 2017 at 14:15 UTC.

has a temperature of about 30° C except little area which located west of Thrace area. It seems that New Tiedtke cumulus physics option produced lowest temperatures for cloud top. Hereunder, North of Thrace region and Black Sea side of European side of Istanbul has about 55° C.

At the second part, New SAS and New Tiedtke produced insignificant amount of hail as output data. KF produced very few hail for Thrace area. the outputs of the model run by KF only shows that the very few hail like 0.1 mm at Thrace region, while MS-KF shows that the amount of hail has 0.5 mm also over the Anatolian side of Istanbul. KF-CuP cumulus option shows that the amount of hail has 1 mm over the Şile region.

In the accumulated rain map, New SAS and New Tiedtke produced insignificant precipitation. KF, MS-KF and KF-CuP cumulus group gave rainfall event over the Thrace region and Bosphorus. MS-KF cumulus option which gives 50 mm accumulated rain from Marmara Sea side of Küçükçekmece to entrance Bosphorus, is the scheme produces highest precipitation.

5.1.3 Sensitivity study with different planetary boundary layer schemes

Two different planetary boundary layer options were identified in the study, YSU and MYNN2. All physical options of the model were held steady and the model was

run again for two different planetary boundary layer options. Model outputs were compared in itself for each planetary boundary layer option. In this way, it was aimed to determine the microphysics scheme which gave the best simulate of the hail event. other physics options are given with Table 5.4.

Table 5.4 : Experiment numbers and options for planetary boundary layer

No	Microphysics	Cumulus	PBL	Sw Rad	Lw Rad
21	Milbrant 2-mom	Kain-Fritsch	YSU	Dudhia	RRTM
22	Milbrant 2-mom	Kain-Fritsch	MYNN2	Dudhia	RRTM

Milbrant 2-mom, Kain Fritsch, Dudhia, RRTM, 38, 41, 1-5, 162, 5 and 30 are used as microphysics, cumulus, shortwave radiation and longwave radiation physics scheme, number of incoming vertical levels, eta levels, surface layer, time step, minutes between cumulus physics call and minutes between cumulus physics, respectively.

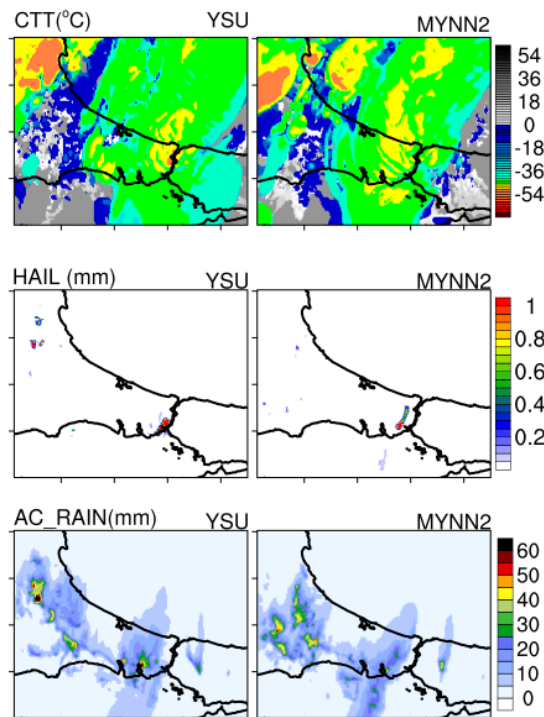


Figure 5.3 : Cloud top temperature($^{\circ}\text{C}$), hail(mm) and accumulated rain(mm) for planetary boundary layers schemes on July 27, 2017 at 14:15 UTC.

Model outputs which run using five different planetary boundary layer options were compared in the same way in Figure 5.3. During the comparison, options were kept constant except for PBL option, and these options are written on maps. At the map showing cloud top temperature, both PBL options produced quite low cloud top temperature over Thrace region.

The outputs of the model run by MYNN2 cumulus option produced more diffused cold regions, while YSU shows that the cloud top temperatures have decreased to as low as -60°C over only Bosphorus and Thrace regions. Also, it is seen that Küçükçekmece and Büyükçekmece region has low temperatures at MYNN option. It is seen that the center of precipitation is located over Bosphorus of the European part of Istanbul and gave about 1mm of hail. YSU also shows another hail formation over the Thrace, while MYNN2 PBL option produced hail over the Marmara Sea near to Küçükçekmece region.

According to accumulated rain map, YSU and MYNN2 produced similar precipitation area for the Thrace region and Anatolian side of Istanbul. The YSU option produced slightly more rain than the MYNN2 option. While the YSU produced 50 mm of rain for Küçükçekmece region, MYNN2 produced about 40 mm of rain.

5.1.4 Sensitivity study with different radiation schemes

Dudhia and RRTMG short-wave radiation options and RRTM and RRTMG long-wave radiation options were identified in the study. All physical options of the model were held steady and the model was run again for two different radiation options. Model outputs were compared in itself for each radiation option. In this way, it was aimed to determine the radiation scheme which gives the best simulate of the hail event. Figure 5.4. Table 5.5.

Table 5.5 : Experiment numbers and options for cumulus

No	Microphysics	Cumulus	PBL	Sw Rad	Lw Rad
22	Milbrant 2-mom	Kain-Fritsch	MYNN2	Dudhia	RRTM
29	Milbrant 2-mom	Kain-Fritsch	MYNN2	RRTMG	RRTMG

5.2 Analysis of the Model Outputs

As a result of comparing six different microphysics, five different cumulus, two different planetary boundary layer, two different short wave radiation and two different long wave radiation physics options, the combination of the physics options of the model that best simulated the hail event has been determined. In this direction, the combination of Milbrant, Kain Fritsch, MYNN2, RRTMG schemes has the best performance.

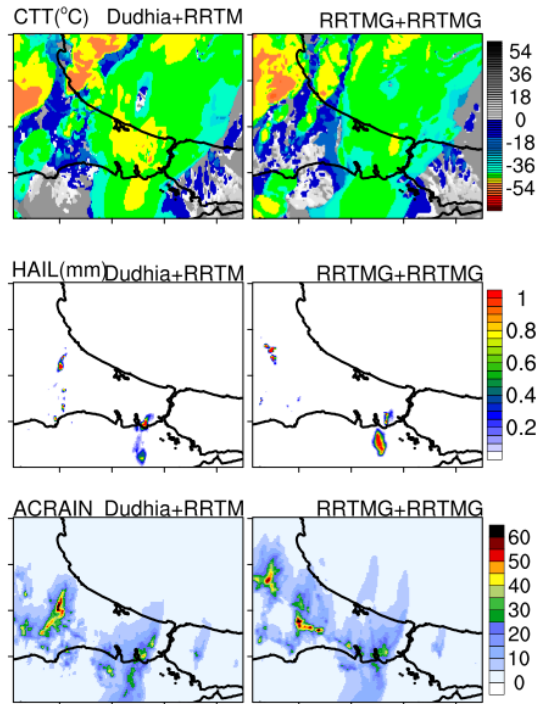


Figure 5.4 : Cloud top temperature($^{\circ}\text{C}$), hail(mm) and accumulated rain(mm) for radiation schemes on July 27, 2017 at 14:15 UTC.

Hail is a quite localised and short-term meteorological event. Therefore, it is quite difficult to simulate the hail phenomenon and to understand its structure. Observational data is insufficient in studying hail formation for lots of case. In order to better interpret the mechanism of hail, temporal and spatial high resolution data are needed. In this study, model outputs at 1 km spatial resolution and at 15-minute temporal resolution were used. It is aimed to understand the hail phenomenon by interpreting the visualized data. The meteorological phenomena such as cloud top temperature, reflectivity, pressure, relative humidity, temperature, wind and precipitation have been analyzed extensively at the output of the model run by these physics options besides cross-section, point and time series analyse.

Each model output data includes 15-minute variables like u-y direction wind speed, accumulated rain, temperature, relative humidity, dew point temperature, sea level pressure. In order to understand the performance of model for hail event, it is necessary to analyze the different time-varying meteorological parameters and compare with observation data. For this reason, station coordinates have been determined and these coordinates have been used to the plot the model data. 15-minute model output pressure, temperature, relative humidity and accumulated precipitation

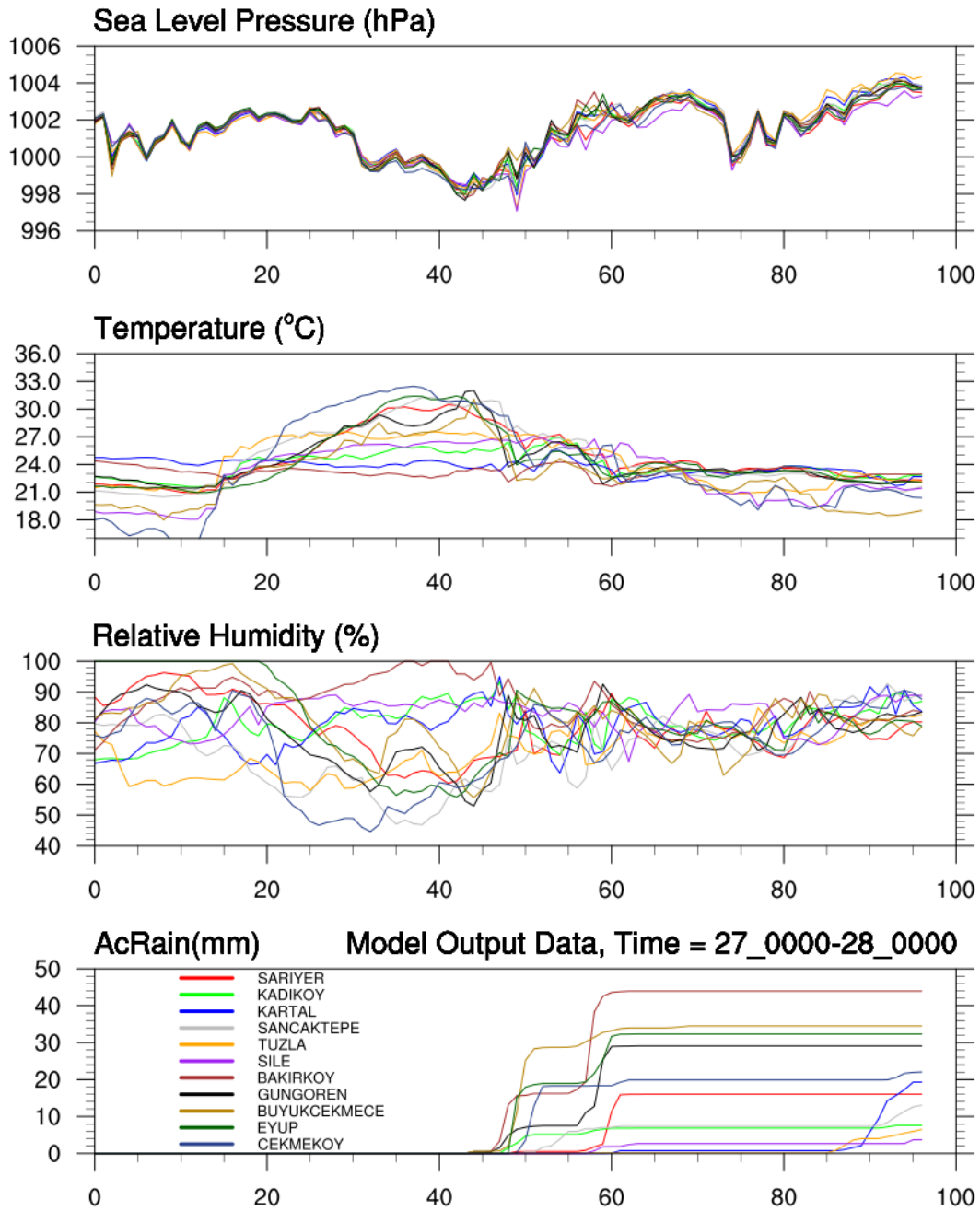


Figure 5.5 : Model results on 11 stations coordinates between 27.07.2017 00:00 UTC and 28.07.2017 00:00 UTC with 15 minutes interval time step.

data between July 27, 2017, 00:00 UTC and July 28, 2017, 00:00 UTC, is shown in Figure 5.5. In the plot, the x-axis shows the time steps in 15-minute intervals and the y-axis shows the variable and its unit. Each of the colored lines represents a different meteorological station which has been used coordinates of. Also the names of these stations are given by bottom legend with the same line colors. The 60th time step shows 14:15 UTC.

When looked at top of the figure, while pressure is decreasing until 998 hPa slightly at the 40th time step, it increased between 40th and 60th time step. After 55th time step, the values became unsteady. After 14:15 UTC pressure increased suddenly. At the second plot, after 55th time step temperature decreased and then values are fixed about 22°C. Relative humidity is quite unstable until 50th time step and became intense about 80% after 14:15 UTC. At the same time step, accumulated rain reached the maximum situation. The accumulated rain data from the model output indicate that rain started at 45th-time step ie at 13:00 UTC and rainfall continued until the night time at some stations coordinates. Precipitation was effective at the time starting at 11:30 UTC and the average amount of rain reached around 25mm. At the end of the day, it is seen that the station with the lowest accumulated precipitation among 11 stations with approximately 2 mm of rain is the Şile region indicated by the purple line. About 40 mm of rain is observed at the Bakırköy station indicated by the maroon line and the maximum accumulated precipitation occurs at this region.

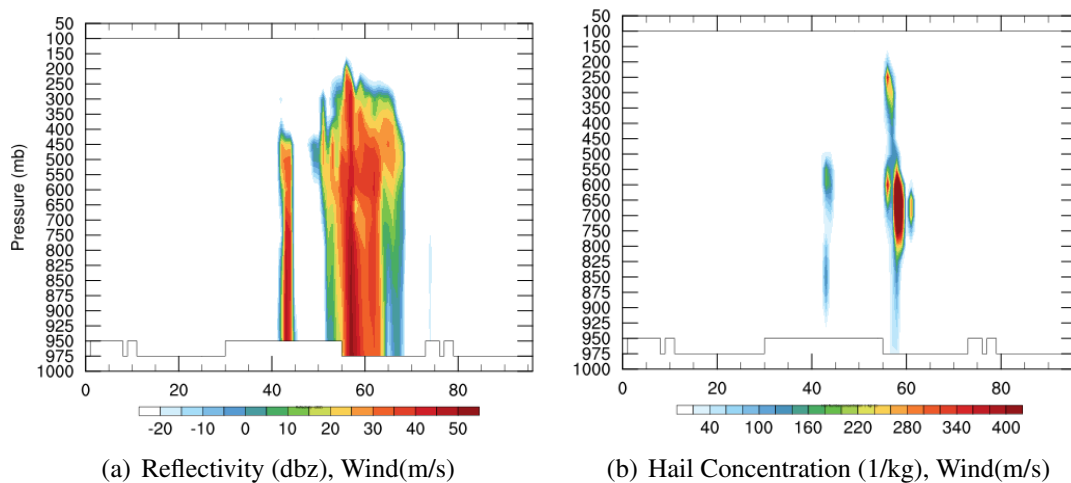


Figure 5.6 : Bakırköy region between 27.07.2017 00:00 UTC and 28.072017 00:00 UTC with 15 minutes interval time step.

One of the most important meteorological phenomena to trigger the formation of hail event is cloud top temperature. Also, reflectivity gives some information about hail concentration and hail structure. Therefore, cloud top temperature and reflectivity were analyzed using model outputs that best simulate hail event. Meteorological parameters such as pressure, relative humidity and temperature were analyzed using model outputs that best simulate hail event. The types of precipitation such as hail and rain were analyzed using model outputs that best simulate hail event. The reflectivity and hail concentration plotted for the place where maximum precipitation occurred,

using model output. This point located on the Bakırköy side of Marmara Sea and is shown in Figure 5.6 for between July 27, 2017, 00:00 UTC and July 28, 2017, 00:00 UTC. In the plot, the x-axis shows the time steps in 15-minute intervals and the y-axis shows the pressure level in mb. The colored areas on the map represent reflectivity in dBZ(a) and hail concentration in 1/kg(b).

According to the figure, the reflectance value between 45-50th time steps and 55-60th time steps is around 50 dBZ from 1000 mb to 300 mb pressure level. Hail concentration is observed at the same time step interval. Maximum hail concentration occurred at around 14:00 UTC with 400/kg.

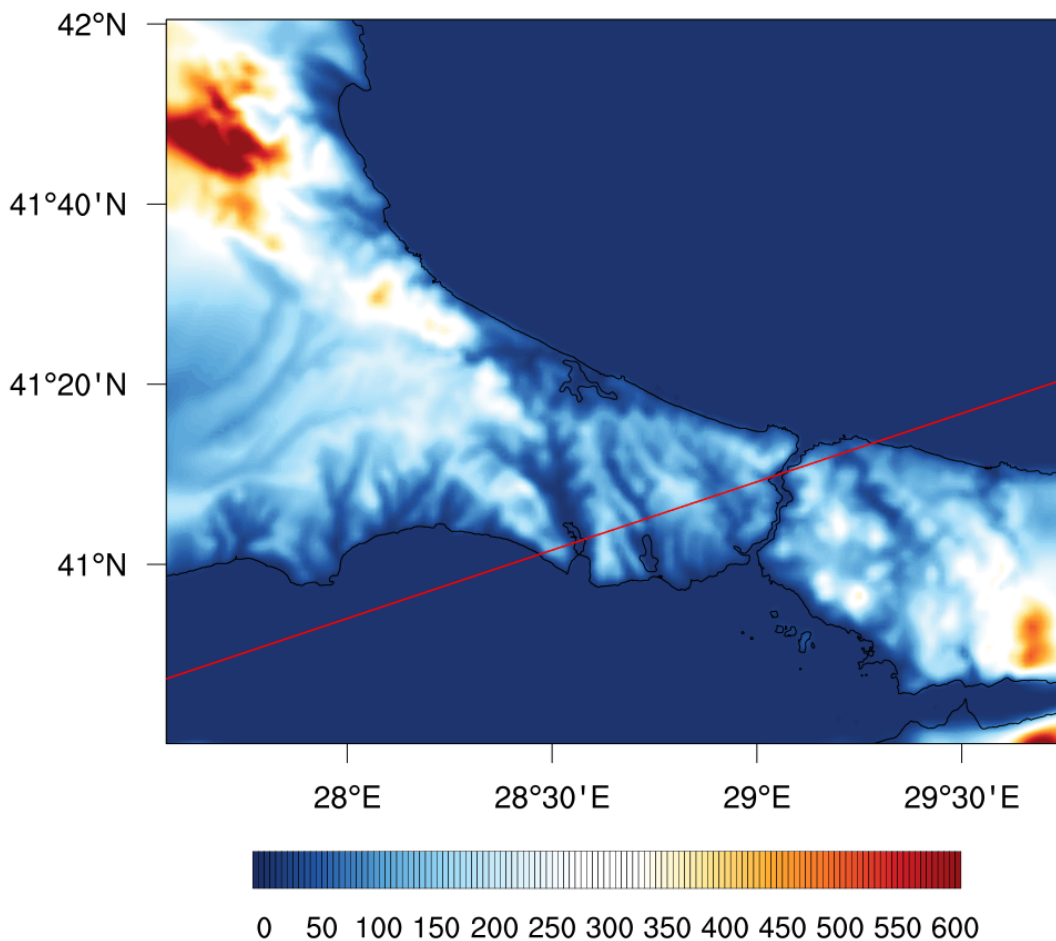


Figure 5.7 : Terrain height(m) and cross-section line for the best model simulation on July 27, 2017 at 14:15 UTC.

A cross-section was taken in the direction of the precipitation system. The points which hail event occurred intensely were determined. The change in meteorological parameters for the day when the hail event was experienced was examined over these crossings and points. Also, meteorological phenomena were analyzed over time series. The cross-section which was determined in the direction of the movement

of the system of the hail event for 27 July 2017 at 14:15 UTC is shown in Figure 5.7. The numbers on the border of the map show the latitude and longitude values of the area determined for the plotting. According to this, the map centred on Istanbul and included some part of Thrace region is located approximately between 40 and 42 North latitudes, between 27 and 30 East longitudes. The coloured areas on the map show terrain height in meters. The colour scale below the map gives the height of the terrain. The height of the land is increasing from blue to red. While the dark blue colour shows areas where the height of terrain is 0 m, in other words, sea level, the red colour shows areas where the height of terrain is 900 m or more. Thick and black contours show land boundaries. Red line shows the cross-section which passed left side Büyükçekmece region. Average terrain height of Cross-section line is 450 m according to terrain map. In addition, the terrain height of Thrace region is about 900 m and this area has the highest terrain values in the map.

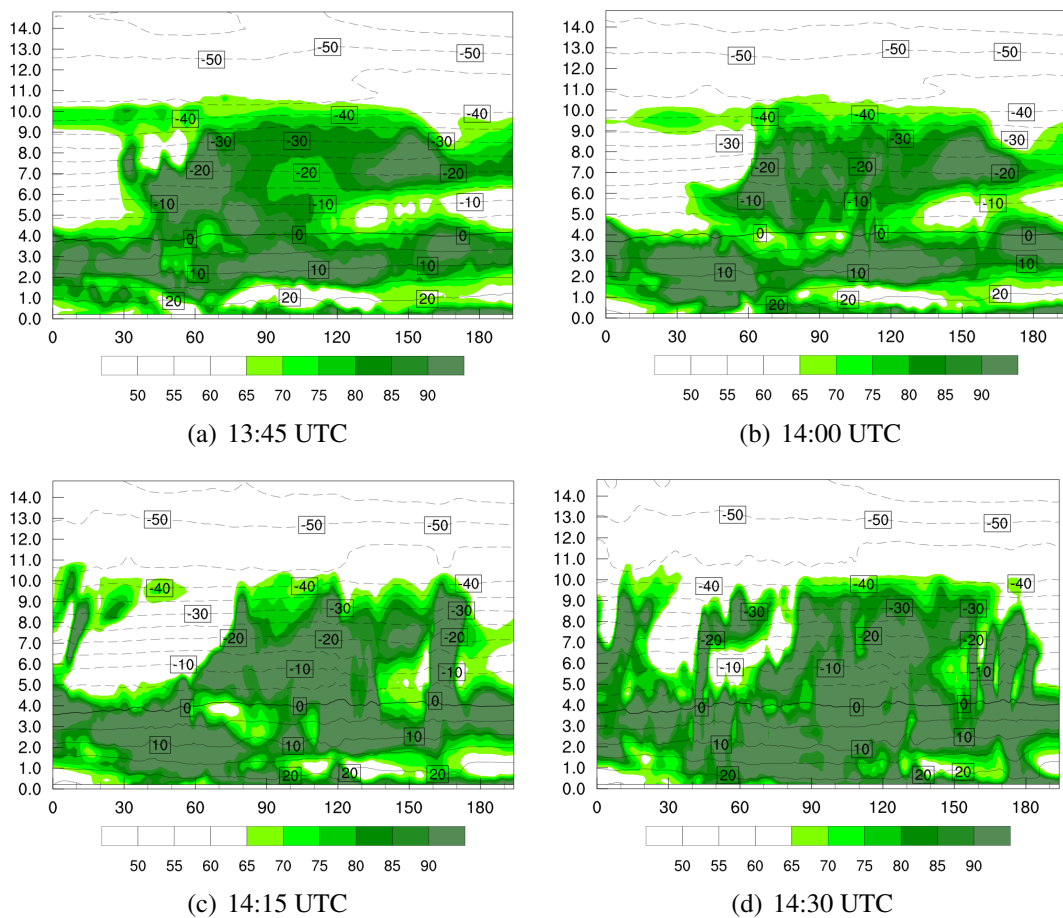


Figure 5.8 : Relative Humidity, Temperature ($^{\circ}\text{C}$) contours of cross-section for the best model simulation on July 27, 2017 at 14:15 UTC.

The relative humidity and temperature which belong to the cross-section were plotted for 13:45, 14:00, 14:15 and 14:30 UTC on July 27, 2017. These plots are shown in Figure 5.8. In this figure, the x-axis shows the grid number of cross-section line from southwest to northeast and the y-axis shows the altitude height in kilometers. The level at which the height is zero km indicates the level of the surface layer. The colored areas on the map show relative humidity in percentage. The color scale below the map gives the percentage of the relative humidity. According to scale, the percentage of the relative humidity is increasing from white to green. The white areas show the relative humidity of 65% or less, the dark green areas show approximately the relative humidity of 90% and higher. Dashed lines indicate temperatures higher than zero, bold line means 0°C, and thin lines are temperatures less than zero. Temperature contours are plotted at 5°C intervals for between -65 and 35 °C. The highest temperature observed in the first 15 kilometers is about 20°C and the lowest temperature is around -55°C. Relative humidity increases over time and spreads to the through the cross section. The white bulge, which appears between 80 and 90 on the x axis, indicates where the land begins. According to this, in the region right of Büyükçekmece, there is 90% humidity in ground level at 14:15 UTC. In the same region, temperature contours approach the surface. The surface level temperatures in this region are decreasing. In this region, amount of relative humidity in the air is 90% from surface level to 10 km height. This ratio is very convenient for cloud formation and precipitation. The temperature in this region is about -40°C at 10 km level. This temperature is suitable for frozen water vapor and hail formation. It is crucial to understand meteorological conditions which cause hail to occur during model performance analysis. In the study, it was examined how the meteorological conditions change during the hail formation by visualizing the model output which is thought to best simulate the 27th July hail event. Deep convective clouds, ascending and descending air movements were plotted by applying three-dimensional visualization to see how the model simulates hail mechanism during the event. Three-dimensional visualizations were prepared by using the VAPOR program supported by The National Center for Atmospheric Research (NCAR). Terrestrial data at a spatial resolution of 500 meters was provided to use for visualization.

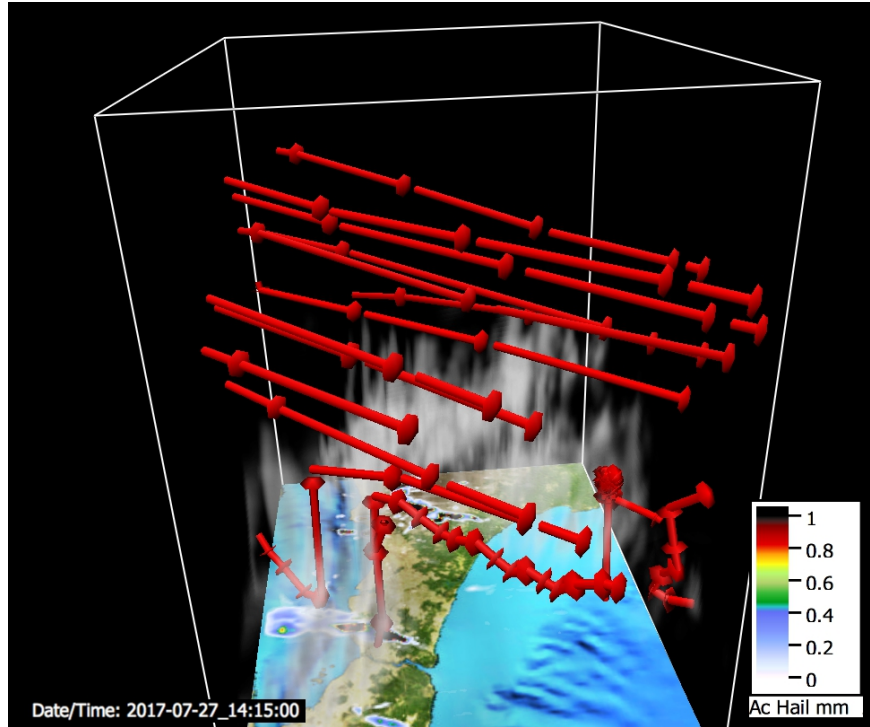


Figure 5.9 : 3D plot of air movement direction on July 27, 2017 at 14:15 UTC.

Air movements and cloudiness which occurred on July 27, 2017, at 14:15 UTC are shown with a three-dimensional plot, in Figure 5.9. The cube surrounded by white lines belongs to the inner domain of the model output and shows the boundaries of the domain in three dimensions. The visual surface on the cube base was formed by high resolution terrestrial data. Blue areas show seas, brown and green areas show land use and land cover. Coloured parts of the land surface that appear like stains show areas where hail occurred. White colour indicates areas in which precipitation occurred weakly, while black colour indicates areas in which precipitation is severe. The thick, red lines in a bar-shaped show the main air movements and wind direction, while the grey areas show the deep convective clouds. According to the air movements, the wind at upper levels is southwesterly, while the dominant wind at the lower levels is southerly generally. At more than one point ascending and descending air movements were observed. The one of the most significant ascending air movement has occurred over the Büyükçekmece region. The air moving in the south-north direction from over the Sea of Marmara has raised on the Büyükçekmece region. Likewise, over the Thrace region, an ascending air movement has occurred inside the clouds. When examined at the surface, the most significant hail events have occurred behind these ascending air movement.

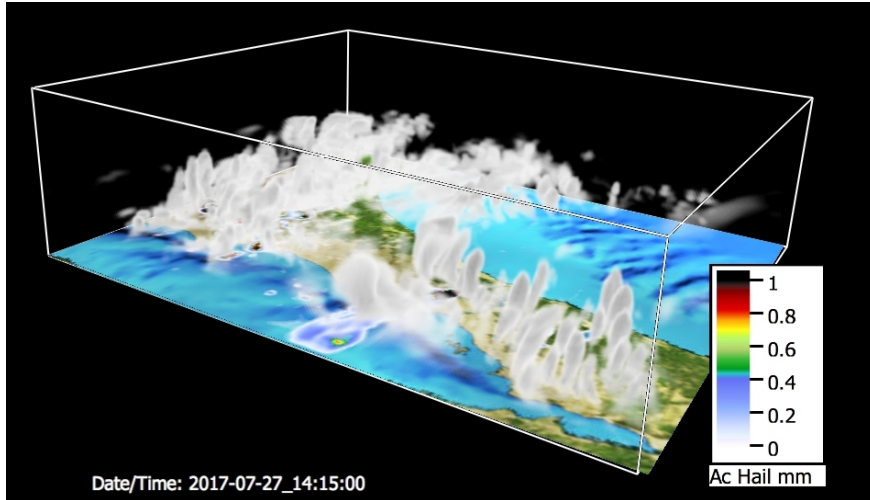


Figure 5.10 : 3D cloudiness(0-1), accumulated hail(mm) for the best model simulation on July 27, 2017 at 14:15 UTC.

Hail event which occurred on July 27, 2017, at 14:15 UTC are shown with a three-dimensional plot, in Figure 5.10. VAPOR visualizer program features were edited to obtain the cloudiness and vertical levels were decreased. The cube surrounded by white lines belongs to the inner domain of the model output and shows the boundaries of the domain in three dimensions. The visual surface on the cube base was formed by high resolution terrestrial data. Blue areas show seas, brown and green areas show land use and land cover. The coloured areas on the map show hail in millimetre. The colour scale on the right side of the map gives the amount of the hail. While the white colour shows areas where the total amount of hail is 0.1 mm or less, the black colour shows areas where the total amount of hail is 1 mm or more. Cloudiness in the region of Thrace is quite high. Similar deep convective clouds are also present in the European side of Bosphorus of Istanbul. According to 3D map in some part of Küçükçekmece region 1 mm hail was observed. 0.8 mm hail has occurred Küçükçekmece side of Marmara Sea.

6. SUMMARY AND CONCLUSION

On July 27, 2017, the hail event over the Istanbul was experienced as a very severe incident, when hundreds of buildings and thousands of vehicles were damaged. At about 12:00 UTC, the hail occurred over Thrace region, and at 15:00 UTC it moved over the Istanbul. 30-40 kg of rainfall was recorded at different points of the city, in the total, as a result of this weather event.

Hail occurs by ascending and descending air movements in deep convective clouds. Hail structure needs temperature between 0 and -40 degrees. In this range of temperature, water droplets freeze and become the supercooled cell. Ice particles touch each other by air movements, become thus enlarged and then create hail. Hail is quite localized and very short time event. Therefore the hail is one of the most difficult predictable meteorological phenomena. Nowadays, it is possible to tracking of hail up with remote sensing technologies and short-term forecasting tools. The case studies, it is shown that increased computer capacity and improved weather forecasting models provide benefits for prediction of meteorological events. Simulations are performed in order to predict the meteorological phenomenon close to reality by using different combinations of the physics options in the model according to the type of the event. The efficiency of prediction methods was analyzed by comparing observations and model outputs. On 27th July 2017 deep convection occurred because of ascending air movements, pressure systems which are located over Europe, and stronger jet winds at mid-latitude in Northern Hemisphere.

The WRF atmosphere model used in the study has an architecture that resolves both the surface and the atmosphere. The high-resolution data can be quickly solved using numerical methods according to the physical options that the user specifies. Before running the WRF model, four nested areas are identified. The outer domain contains Balkans and a large part of Turkey and has 27 km spatial resolution. The second domain contains Marmara Region and Thrace and has 9 km spatial resolution. The third domain contains Istanbul and some part of Thrace region and has 3 km

spatial resolution. The innermost domain contains Istanbul and has 1 km spatial resolution. The temporal resolutions of the outputs obtained for the four identified areas are 15 minutes for the innermost area and 180 minutes for the outer areas. ERA-Interim reanalysis data for 38 different pressure levels with 0.75x0.75 spatial and 6-hour temporal resolution is preferred to give to model as input data. In order to compare with the model results, observation data obtained from meteorological stations, satellite and radar has taken from Turkish State Meteorological Service. YSU and MYNN2 is chosen for PBL schemes; New SAS, Multi Scale KF, KF-Cup and New Tiedtke are chosen for cumulus schemes; Lin, Milbrandt 2-mom, NSSL 2-mom, Kain Fritsch, New SAS and Multi Scale KF are chosen for microphysics schemes; Dudhia and RRTMG are chosen for short-wave radiation schemes and RRTM and RRTMG are chosen for long-wave radiation schemes. Then, combinations of these physics options are performed to evaluate parameterization effect for the case study. All different simulation output were compared with observational data.

The thesis is focused on determining the combination of the physics options that improve the hail simulations with WRF. During the processe sensitivity tests were performed. According to results of the study, the combination of Milbrandt, Kain Fritsch, MYNN2, RRTMG schemes has the best performance amongst all the sensitivity tests. According to the best model outputs, accumulated precipitation is 40 mm from 27 July to 28 July; hail event starts at 14:15 UTC; and the cloud top temperature over Istanbul is about -50°C at the same time. Deep convective clouds reaches about 12 km height. Maximum hail concentration is about 400/kg at 14:15 UTC; and it occurs at about 500mb pressure level. Reflectivity is about 50 dBZ when hail event occurred.

Inconsistencies were experienced during the comparison of the observation data with the model outputs due to the low sensitivity of the precipitation sensor to hail event. The total accumulated precipitation obtained from model outputs is more than the observed data.

REFERENCES

- [1] **Gray, W.M. and Jacobson, R.W.** (1977). Diurnal Variation of Deep Cumulus Convection, *105*(9), 1171–1188.
- [2] **Browning, K.A., Frankhauser, J.C., Chalon, J.P., Eccles, P.J., Strauch, R.G., Merrem, F.H., Musil, D.J., May, E.L. and Sand, W.R.** (1976). Structure of an evolving hailstorm part V: Synthesis and implications for hail growth and hail suppression, *104*(5), 603–610.
- [3] **Knight, C.A. and Knight, N.C.** (1970). The Falling Behavior of Hailstones, *27*(4), 672–681.
- [4] **Amburn, S.a. and Wolf, P.L.** (1997). VIL Density as a Hail Indicator, *Weather and Forecasting*, *12*(3), 473–478.
- [5] **Knight, N.C.** (1981). The Climatology of Hailstone Embryos, *20*(7), 750–755.
- [6] **Nelson, S.P.** (1983). The Influence of Storm Flow Structure on Hail Growth, *40*, 1965–1983.
- [7] **Ronald, E.R.** (1997). *Radar for meteorologists*, Rinehart publishing.
- [8] **Balakrishnan, N. and Zrnić, D.S.** (1990). Estimation of Rain and Hail Rates in Mixed-Phase Precipitation, *47*(5), 565–587.
- [9] **Auer Jr., A.H.** (1994). Hail Recognition Through the Combined Use of Radar Reflectivity and Cloud-Top Temperature, *122*, 2218–2221.
- [10] **Kahraman, A., Tilev-Tanriover, e., Kadioglu, M., Schultz, D.M. and Markowski, P.M.** (2016). Severe Hail Climatology of Turkey, *Monthly Weather Review*, *144*(1), 337–346.
- [11] **Reddy, M.V., Prasad, S.B., Krishna, U.V. and Reddy, K.K.** (2014). Effect of cumulus and microphysical parameterizations on the JAL cyclone prediction, *Indian Journal of Radio and Space Physics*, *43*(1), 103–123.
- [12] **Weisman, M.L., Davis, C., Wang, W., Manning, K.W. and Klemp, J.B.** (2008). Experiences with 0?36-h Explicit Convective Forecasts with the WRF-ARW Model, *Weather and Forecasting*, *23*(3), 407–437.
- [13] **Morrison, H., Milbrandt, J.A., Bryan, G.H., Ikeda, K., Tessendorf, S.A. and Thompson, G.** (2015). Parameterization of Cloud Microphysics Based on the Prediction of Bulk Ice Particle Properties. Part II: Case Study Comparisons with Observations and Other Schemes, *Journal of the Atmospheric Sciences*, *72*(1), 312–339.

- [14] **Li, X., Zhang, Q. and Xue, H.** (2017). The role of initial cloud condensation nuclei concentration in hail using the WRF NSSL 2-moment microphysics scheme, *Advances in Atmospheric Sciences*, 34(9), 1106–1120.
- [15] **Adams-Selin, R.D. and Ziegler, C.L.** (2016). Forecasting Hail Using a One-Dimensional Hail Growth Model within WRF, *Monthly Weather Review*, 144(12), 4919–4939.
- [16] **Agnihotri, G. and Dimri, A.P.** (2015). Simulation study of heavy rainfall episodes over the southern Indian peninsula, *Meteorological Applications*, 22(2), 223–235.
- [17] **Tian, J., Liu, J., Wang, J., Li, C., Yu, F. and Chu, Z.** (2017). A spatio-temporal evaluation of the WRF physical parameterisations for numerical rainfall simulation in semi-humid and semi-arid catchments of Northern China, *Atmospheric Research*, 191, 141–155.
- [18] **Chevuturi, A., Dimri, A.P. and Gunturu, U.B.** (2014). Numerical simulation of a rare winter hailstorm event over Delhi, India on 17 January 2013, *Natural Hazards and Earth System Sciences*, 14(12), 3331–3344.
- [19] **Dasari, H.P. and Salgado, R.** (2015). Numerical modelling of heavy rainfall event over Madeira Island in Portugal: Sensitivity to different micro physical processes, *Meteorological Applications*, 22(1), 113–127.
- [20] **Chawla, I., Osuri, K.K., Mujumdar, P.P. and Niyogi, D.** (2017). Assessment of the Weather Research and Forecasting (WRF) Model for Extreme Rainfall Event Simulations in the Upper Ganga Basin, *Hydrology and Earth System Sciences*, (August), 1–29.
- [21] **Murthy, B.S., Latha, R. and Madhuparna, H.** (2018). WRF simulation of a severe hailstorm over Baramati: a study into the space?time evolution, *Meteorology and Atmospheric Physics*, 130(2), 153–167.
- [22] **Lin, Y.L., Farley, R.D. and Orville, H.D.,** Bulk Parameterization of the Snow Field in a Cloud Model.
- [23] **Milbrandt, J.A. and Yau, M.K.** A Multimoment Bulk Microphysics Parameterization. Part I: Analysis of the Role of the Spectral Shape Parameter, *Journal of the Atmospheric Sciences*, (9), 3051–3064.
- [24] **Milbrandt, J.A. and Yau, M.K.** A Multimoment Bulk Microphysics Parameterization. Part II: A Proposed Three-Moment Closure and Scheme Description, *Journal of the Atmospheric Sciences*, (9), 3065–3081.
- [25] **Tao, W.K., Simpson, J. and McCumber, M.,** An Ice-Water Saturation Adjustment.
- [26] **Mansell, E.R., Ziegler, C.L. and Bruning, E.C.** Simulated Electrification of a Small Thunderstorm with Two-Moment Bulk Microphysics, *Journal of the Atmospheric Sciences*, (1), 171–194.

- [27] **Kain, J.S.** The Kain-Fritsch Convective Parameterization: An Update, *Journal of Applied Meteorology*, (1), 170–181.
- [28] **Han, J. and Pan, H.L.** Revision of Convection and Vertical Diffusion Schemes in the NCEP Global Forecast System, *Weather and Forecasting*, (4), 520–533.
- [29] **Zheng, Y., Alapaty, K., Herwehe, J.A., Del Genio, A.D. and Niyogi, D.** Improving High-Resolution Weather Forecasts Using the Weather Research and Forecasting (WRF) Model with an Updated Kain-Fritsch Scheme, *Monthly Weather Review*, (3), 833–860.
- [30] **Ma, L.M. and Tan, Z.M.** Improving the behavior of the cumulus parameterization for tropical cyclone prediction: Convection trigger, *Atmospheric Research*, (2), 190–211.
- [31] **Tiedtke, M.**, A Comprehensive Mass Flux Scheme for Cumulus Parameterization in Large-Scale Models.
- [32] **Hong, S.Y., Noh, Y. and Dudhia, J.** A New Vertical Diffusion Package with an Explicit Treatment of Entrainment Processes, *Monthly Weather Review*, (9), 2318–2341.
- [33] **Nakanishi, M. and Niino, H.** (2006). An improved Mellor-Yamada Level-3 model: Its numerical stability and application to a regional prediction of advection fog, *Boundary-Layer Meteorology*, 119(2), 397–407.
- [34] **NAKANISHI, M. and NIINO, H.** Development of an Improved Turbulence Closure Model for the Atmospheric Boundary Layer, *Journal of the Meteorological Society of Japan*, (5), 895–912.
- [35] **Dudhia, J.**, Numerical Study of Convection Observed during the Winter Monsoon Experiment Using a Mesoscale Two-Dimensional Model.
- [36] **Iacono, M.J., Delamere, J.S., Mlawer, E.J., Shephard, M.W., Clough, S.A. and Collins, W.D.** (2008). Radiative forcing by long-lived greenhouse gases: Calculations with the AER radiative transfer models, *Journal of Geophysical Research Atmospheres*, 113(13), 2–9.
- [37] **Mlawer, E.J., Taubman, S.J., Brown, P.D., Iacono, M.J. and Clough, S.A.** Radiative transfer for inhomogeneous atmospheres: RRTM, a validated correlated-k model for the longwave, *Journal of Geophysical Research: Atmospheres*, (D14), 16663–16682.

APPENDICES

APPENDIX A.1 : NCL Code for Cloud Top Temperature, Hail and Accumulated Rain

APPENDIX A.1

```
load ".../csm/gsn_code.ncl"
load ".../csm/gsn_csm.ncl"
load ".../wrf/WRFUserARW.ncl"
.....
begin
a = addfile("runa/wrfoutd042017-07-26180000","r")
b = addfile("runb/wrfoutd042017-07-26180000","r")
c = addfile("runc/wrfoutd042017-07-26180000","r")
d = addfile("rund/wrfoutd042017-07-26180000","r")
e = addfile("rune/wrfoutd042017-07-26180000","r")
type = "png"
wks = gsnopenwks(type,"Cufark")
res = True
pnlres = True
pnlres@PanelPlot = True
mpres = True
pnlres1 = True
pnlres1@PanelPlot = True
pnlres2 = True
pnlres2@PanelPlot = True
pnlres3 = True
pnlres3@PanelPlot = True
.....
function cttpal()
local cmap
begin
cmap = (/ (/ 100, 0, 0/), (/ 200, 0, 0/), (/ 255, 0, 0/), (/ 255, 100, 30/),
(/ 255, 128, 65/), (/ 255, 255, 0/), (/ 0, 255, 0/), (/ 0, 255, 200/),
(/ 0, 225, 225/), (/ 0, 225, 225/), (/ 0, 150, 200/), (/ 0, 100, 200/),
(/ 0, 100, 200/), (/ 0, 0, 200/), (/ 0, 0, 200/), (/ 0, 0, 200/),
(/ 250, 250, 250/), (/ 230, 230, 230/), (/ 210, 210, 210/),
```

```

(/ 190, 190, 190/), (/ 170, 170, 170/), (/ 150, 150, 150/),
(/ 130, 130, 130/), (/ 110, 110, 110/), (/ 90, 90, 90/),
(/ 70, 70, 70/), (/ 50, 50, 50/), (/ 20, 20, 20/), (/ 10, 10, 10/), (/ 0, 0, 0/ ) /255.
return(cmap)
end
.....
mpres@tfDoNDCOverlay = True ; set True for native (direct) mapping
mpres@mpProjection = "Mercator"
mpres@mpDataBaseVersion = "HighRes"
mpres@mpGeophysicalLineThicknessF = 4.
mpres@mpGeophysicalLineColor = "black"
mpres@tmXBLabelsOn = False
mpres@tmYLLLabelsOn = False
.....
times = wrfusergetvar(a,"times",-1) ; get all times in the file
ntimes = dimsizes(times)
i = 81 ; for 14:15 UTC
print(times(i))
restot = True
restot@gsnFrame = False
restot@gsnDraw = False
restot@gsnFrame = False ; do not advance frame
restot@cnFillOn = True
restot@cnFillMode = "RasterFill"
restot@cnFillPalette = "WhB1GrYeRe"
restot@cnLinesOn = False ; turn off contour lines
restot@cnFillOpacityF = 1. ; .85
restot@tfDoNDCOverlay = True ; necessary for correct overlay on map
restot@cnLevelSelectionMode = "ManualLevels"
restot@cnMaxLevelValF = 1
restot@cnMinLevelValF = 0.05
restot@cnLevelSpacingF = 0.05
restot@lbLabelBarOn = False ; Turn off individual labelbars so we can
restot@cnInfoLabelOn = False

```

```

restot@gsnRightStringFontHeightF = 0.05
restot@gsnLeftStringFontHeightF = 0.05
:
HailMomenta = a->HAILNC(i,,:)-a->HAILNC(i-1,,:);
HailMomentb = b->HAILNC(i,,:)-b->HAILNC(i-1,,:);
HailMomentc = c->HAILNC(i,,:)-c->HAILNC(i-1,,:);
HailMomentd = d->HAILNC(i,,:)-d->HAILNC(i-1,,:);
HailMomente = e->HAILNC(i,,:)-e->HAILNC(i-1,,:);
restot@tiMainString = ""
restot@gsnLeftString = "HAIL(mm)"
restot@gsnRightString = "KF"
plothaia = gsncsmcontour(wks,HailMomenta,restot)
plot1 = wrfmapoverlays(a,wks,plothaia,pnlres,mpres)
restot@gsnLeftString = ""
restot@gsnRightString = "New SAS"
plothaib = gsncsmcontour(wks,HailMomentb,restot)
plot2 = wrfmapoverlays(b,wks,plothaib,pnlres,mpres)
restot@gsnRightString = "MS-KF"
plothaic = gsncsmcontour(wks,HailMomentc,restot)
plot3 = wrfmapoverlays(c,wks,plothaic,pnlres,mpres)
restot@gsnRightString = "KF-CuP"
plothaidd = gsncsmcontour(wks,HailMomentd,restot)
plot4 = wrfmapoverlays(d,wks,plothaidd,pnlres,mpres)
restot@gsnRightString = "New Tiedtke"
plothaie = gsncsmcontour(wks,HailMomente,restot)
plot5 = wrfmapoverlays(e,wks,plothaie,pnlres,mpres)
:
ctta = wrfusergetvar(a,"ctt",i)
cttb = wrfusergetvar(b,"ctt",i)
cttc = wrfusergetvar(c,"ctt",i)
cttd = wrfusergetvar(d,"ctt",i)
ctte = wrfusergetvar(e,"ctt",i)
opts = True
opts@gsnFrame = False

```

```

opts@gsnDraw = False
opts@cnLinesOn = False ; turn off contour lines
opts@cnLineLabelsOn = False ; turn off contour labels
opts@cnFillOpacityF = 1. ; .85
opts@tfDoNDCOverlay = True ; necessary for correct overlay on map
opts@lbLabelBarOn = False ; Turn off individual labelbars so we can
opts@cnFillOn = True
opts@cnFillMode = "RasterFill"
opts@cnFillPalette = cttpal()
opts@cnLevelSelectionMode = "ManualLevels"
opts@cnMaxLevelValF = 60
opts@cnMinLevelValF = -70
opts@cnLevelSpacingF = 2.
opts@gsnSpreadColorEnd = -1 ; End third from the last color in color map
opts@ValidTime = False
opts@InitTime = False
opts@Footer = False
opts@gsnMaximize = True
opts@NoHeaderFooter = True
pnlres@NoTitles = True ; Turn off the left title just above the plot
pnlres@CommonTitle = True ; Replace description (units) title with our own title
pnlres@FontHeightF = .012
pnlres@PlotTitle = "CTT( S o N C) KF"
contourctta = wrf_contour(a,wks,ctta,opts)
plot6 = wrf_mapoverlays(a,wks,contourctta,pnlres,mpres)
pnlres@PlotTitle = " New SAS"
contourcttb = wrf_contour(b,wks,cttb,opts)
plot7 = wrf_mapoverlays(b,wks,contourcttb,pnlres,mpres)
pnlres@PlotTitle = " MS-KF"
contourcttc = wrf_contour(c,wks,cttc,opts)
plot8 = wrf_mapoverlays(c,wks,contourcttc,pnlres,mpres)
pnlres@PlotTitle = " KF-CuP"
contourcttd = wrf_contour(d,wks,cttd,opts)
plot9 = wrf_mapoverlays(d,wks,contourcttd,pnlres,mpres)

```

```

pnlres@PlotTitle = " New Tiedtke"
contourctte = wrfcontour(e,wks,ctte,opts)
plot10 = wrfmapoverlays(e,wks,contourctte,pnlres,mpres)
pnlres@CommonTitle = False ; Replace description (units) title with our own title
.....
raintot = True
raintot@gsnFrame = False
raintot@gsnDraw = False
raintot@gsnFrame = False ; do not advance frame
cmap := readcolormapfile("precip217lev")
cmap(0,:) = (/0,0,0,0/) ; make first color fully transparent
raintot@cnFillOn = True
raintot@cnFillMode = "RasterFill"
raintot@cnFillPalette = cmap
raintot@cnLinesOn = False ; turn off contour lines
raintot@cnLineLabelsOn = False ; turn off contour labels
raintot@cnFillOpacityF = 1. ; .85
raintot@tfDoNDCOverlay = True ; necessary for correct overlay on map
raintot@cnLevelSelectionMode = "ManualLevels"
raintot@cnMaxLevelValF = 60
raintot@cnMinLevelValF = 0
raintot@cnLevelSpacingF = 5
raintot@lbLabelBarOn = False ; Turn off individual labelbars so we can
raintot@tiMainString = ""
raintot@gsnCenterString = ""
raintot@gsnRightString = "" ; assign right string
raintot@gsnLeftString = ""
raintot@gsnRightStringFontHeightF = 0.05
raintot@gsnLeftStringFontHeightF = 0.05
raintot@cnInfoLabelOn = False
.....
RAINMomenta = a->RAINNC(i,:,:)
RAINMomentb = b->RAINNC(i,:,:)
RAINMomentc = c->RAINNC(i,:,:)

```

```

RAINMomentd = d->RAINNC(i,,:)
RAINMomete = e->RAINNC(i,,:)
raintot@gsnLeftString = "ACRAIN(mm)"
raintot@gsnRightString = "KF"
plotRAINa = gsncsmcontour(wks,RAINMomenta,raintot)
plot16 = wrfmapoverlays(a,wks,plotRAINa,pnlres,mpres)
raintot@gsnLeftString = ""
raintot@gsnRightString = "New SAS"
plotRAINb = gsncsmcontour(wks,RAINMomentb,raintot)
plot17 = wrfmapoverlays(b,wks,plotRAINb,pnlres,mpres)
raintot@gsnRightString = "MS-KF"
plotRAINc = gsncsmcontour(wks,RAINMomentc,raintot)
plot18 = wrfmapoverlays(c,wks,plotRAINc,pnlres,mpres)
raintot@gsnRightString = "KF-CuP"
plotRAINd = gsncsmcontour(wks,RAINMomentd,raintot)
plot19 = wrfmapoverlays(d,wks,plotRAINd,pnlres,mpres)
raintot@gsnRightString = "New Tiedtke"
plotRAINe = gsncsmcontour(wks,RAINMomete,raintot)
plot20 = wrfmapoverlays(e,wks,plotRAINe,pnlres,mpres)
.....
pnlres1@txString = "/ KF / New SAS / MS-KF / KF-CuP / New Tiedtke / " +
chartostring(a->Times(i,:))
; CTT
pnlres1@gsnPanelYWhiteSpacePercent = 2 ; Add white space b/w plots.
pnlres1@gsnPanelLabelBar = True ; Turn on common labelbar
pnlres1@lbLabelAutoStride = True ; Spacing of lbar labels.
pnlres1@gsnFrame = False ; save panel until both ready
pnlres1@gsnPanelBottom = 0.7
pnlres1@lbOrientation = "vertical"
pnlres1@lbLabelFontHeightF = 0.012 ; LABEL NUMBERS FONT
pnlres1@pmLabelBarWidthF = 0.04 ; default is shorter
pnlres1@pmLabelBarHeightF = 0.14
; RAIN
pnlres2@gsnPanelYWhiteSpacePercent = 2 ; Add white space b/w plots.
pnlres2@gsnPanelLabelBar = True ; Turn on common labelbar

```

```

pnlres2@lbLabelAutoStride = True ; Spacing of lbar labels.
pnlres2@gsnFrame = False ; save panel until both ready
pnlres2@gsnPanelTop = 0.87
pnlres2@lbOrientation = "vertical"
pnlres2@lbLabelFontHeightF = 0.012
pnlres2@pmLabelBarWidthF = 0.04 ; default is shorter
pnlres2@pmLabelBarHeightF = 0.14
; HAIL
pnlres3@gsnPanelYWhiteSpacePercent = 2 ; Add white space b/w plots.
pnlres3@gsnPanelLabelBar = True ; Turn on common labelbar
pnlres3@lbLabelAutoStride = True ; Spacing of lbar labels.
pnlres3@gsnFrame = False ; save panel until both ready
pnlres3@gsnPanelBottom = 0.25
pnlres3@lbOrientation = "vertical"
pnlres3@lbLabelFontHeightF = 0.013
pnlres3@pmLabelBarWidthF = 0.04 ; default is shorter
pnlres3@pmLabelBarHeightF = 0.14
gsnpanel(wks,(/plot1,plot2,plot3,plot4,plot5/),(/1,5/),pnlres3)
gsnpanel(wks,(/plot6,plot7,plot8,plot9,plot10/),(/1,5/),pnlres1)
gsnpanel(wks,(/plot16,plot17,plot18,plot19,plot20/),(/1,5/),pnlres2)
frame(wks)
:
end

```

CURRICULUM VITAE



Name Surname:

Emir Toker

Place and Date of Birth:

Istanbul, Turkey 30 November 1990

E-Mail:

tokerem@itu.edu.tr

EDUCATION:

- **B.Sc.:** 2016, Istanbul Technical University, Faculty of Aeronautics and Astronautics, Meteorological Engineering

PROFESSIONAL EXPERIENCE AND REWARDS:

- Sept 2014 - Sept 2015, Polat Energy, Wind Measurement and Assessment Department, Long-Term Internship, Istanbul, Turkey
- 23 - 27 April 2018, European Centre for Medium-Range Weather Forecasts, Parametrization of Subgrid Physical Processes, Training, Reading, UK
- 30 Apr - 4 May 2018, European Centre for Medium-Range Weather Forecasts, Predictability and ensemble forecast systems, Training, Reading, UK

PUBLICATIONS, PRESENTATIONS AND PATENTS ON THE THESIS:

- **Toker, E., Lütfi, Ö. Ş., Ezber, Y.,** 2018. Performance of WRF in Simulating the Hail Event over Istanbul on 27 July 2017. *Scientific Congress of The Turkish National Union of Geodesy and Geophysics (TUJJBK)*, May 30 - June 2, 2018 Izmir, Turkey.
- **Toker, E., Lütfi, Ö. Ş., Ezber, Y.,** 2018. Performance of WRF in Simulating the Hail Event over Istanbul on 27 July 2017. *Quaternary Symposium of Turkey (TURQUA)*, May 2-5, 2018 Istanbul, Turkey.
- **Toker, E., Lütfi, Ö. Ş., Ezber, Y.,** 2018. Performance of WRF in Simulating the Hail Event over Istanbul on 27 July 2017. *European Geosciences Union General Assembly (EGU)*, April 8-13, 2018 Vienna, Austria.